

UNCLASSIFIED

AD 271 599

*Reproduced
by the*

**ARMED SERVICES TECHNICAL INFORMATION AGENCY
ARLINGTON HALL STATION
ARLINGTON 12, VIRGINIA**



UNCLASSIFIED

NOTICE: When government or other drawings, specifications or other data are used for any purpose other than in connection with a definitely related government procurement operation, the U. S. Government thereby incurs no responsibility, nor any obligation whatsoever; and the fact that the Government may have formulated, furnished, or in any way supplied the said drawings, specifications, or other data is not to be regarded by implication or otherwise as in any manner licensing the holder or any other person or corporation, or conveying any rights or permission to manufacture, use or sell any patented invention that may in any way be related thereto.

CATALOGED BY ASTIA
AS AD NO. **274 599**

62-2-2
NOX



ASTIA
RECEIVED
FEB 15 1962
TISIA A

821960

**INVESTIGATION OF OPTICAL COATINGS
FOR SOLAR CELLS**

**Report No. 1, First Semi-Annual Report
25 January 1960 through 30 June 1960
Contract No. DA 36-039 SC-85284
Signal Corps Contract No. 85284
ARPA Order No. 80-59**

**U. S. Army Signal Research and Development
Laboratory - Fort Monmouth, New Jersey**

**Prepared Under the Direction of
A. E. Mann, Senior Physicist**

**OBJECT: Evaluation of State-of-the-Art
Coatings for Silicon Cells and Advances
towards the Idealized "Window Coating"
which would Optimize Temperature Reduction**



TABLE OF CONTENTS

Section 1	PURPOSE	2
2	ABSTRACT	4
3	PUBLICATIONS, LECTURES, REPORTS AND CONFERENCES	5
4	FACTUAL DATA	6
	TASK ONE: Thermal Analysis of Spectrally Selective Cell Coatings	6
	TASK TWO: Evaluation of State-of-the-Art Coatings	15
	TASK THREE: Adaptation of Window Coatings to Solar Cells	21
5	CONCLUSIONS	25
6	PROGRAM FOR THE NEXT INTERVAL	26
7	IDENTIFICATION OF KEY TECHNICAL PERSONNEL	27
TEST NO. I	HUMIDITY	
II	HIGH TEMPERATURE	
III	LOW TEMPERATURE	
IV	TEMPERATURE CYCLE	
V	VACUUM	
FIGURE 1	Schematic of Coated Silicon Cell, Glass Type Coating	
2	Schematic of Coated Silicon Cell, Direct Coating	
3	Photograph of Typical Coated Cell Array	
4	Relative Solar Spectral Irradiance	
5	Spectral Emissivity of Typical Silicon Solar Cell (Uncoated)	
6	Spectral Emissivity for Black Body at 50°C	
7	Maximum Power Versus Temperature for Typical Silicon Solar Cell	
8	Solakote A/40 Transmittance	
9	Solakote B 2/0/470 Transmittance	
10	OCLI Cell Cover Slip Type 207 SCC 460 Transmittance	
11	Solar Cell Window Transmittance	
12	Solar Cell Window Coating Transmittance	
13	Spectral Emissivity of Typical Silicon Solar Cell with Solakote A, D, C, and D	

Table of Contents - Page 2

FIGURE 14	Typical Spectral Transmittance of Solakote B Solar Cell Coating (470 mμ cutoff)
15	Relative Spectral Sensitivity of Typical Silicon Solar Cell
16	tE Product Curves for Blue-Violet Reflecting Filter
17	tE Product Curves for "Window Coating"
18	Equilibrium Temperatures for Typical Solar Panel
19	Equilibrium Temperature Versus Solar Irradiance (Air-Mass-Zero)
20	Resultant Coated Panel Output for Three Coating Types in Orbits near Venus, Earth and Mars
21	Spectrolab Type A-42 Coating Transmission
22	Spectrolab Type B 1/S/460 Coating Transmission
23	Spectrolab Type B 2/O/470 Coating Transmission
24	OCLI Type 207 SCC 460 Coating Transmission
25	Fish-Schurman Type 3119 Coating Transmission
26	Fish-Schurman Type 3119 Published Transmission
27	Infrared Reflectance of Typical Cell with Solakote A-40 Coating
28	Infrared Reflectance of Typical Cell with Solakote B 2/O Coating
29	Infrared Reflectance of Typical Cell with OCLI 207 SCC Coating
30	Schematic Diagram of Ultraviolet Test Apparatus
31	Photograph of Ultraviolet Test Apparatus
32	Photograph of Typical Panel After Completion of Test Sequence
33	Nine-Layer ADI Filter Curve
34	Long Wave Reflector Curve
35	Optical Films of Rare Earth Salts
36	Window Coating Transmittance

Section 1

PURPOSE

This research program is concerned with the investigation of coatings for increasing efficiency of and providing protection to silicon solar cells used for converting solar energy into electrical energy for space power systems. Such photovoltaic conversion of solar energy has evolved as the primary state-of-the-art source of auxiliary power for small and intermediate space vehicles. The advantages of solar energy for such purposes are well known and will not be discussed here.

In the United States, 1 by 2 cm p-on-n silicon cells are currently being used for almost all space power systems. Spectrally selective coatings are applied to the cell surfaces to reduce the operating temperature, increase efficiency, and to provide protection against mechanical damage, surface contamination, micro-meteorite erosion and beta radiation.

These cell coatings may be applied either directly to the cell surface or to thin glass slips which are, in turn, bonded to the cells. This latter class provides maximum protection against the various environmental hazards and are, therefore, being used almost exclusively in current space programs. The type and thickness of glass depends upon the mission, and may vary from 3 mil microsheet to 70 mil radiation resistant formulations. The two varieties of cell coatings are schematically illustrated in Figures 1 and 2 below. In Figure 3 is shown a photograph of a typical coated cell array.

Although these protective properties are of extreme importance, the primary purpose of the coatings is to increase conversion efficiency by reduction of operating temperature. The temperature degradation of silicon cells is well known. Materials having higher energy gaps than silicon might be expected to have better thermal characteristics, but experimental evidence indicates that for current

cells the difference is small because the rate of minority carrier generation goes up faster than is predicted from energy gap considerations alone. The problem of thermal degradation of photovoltaic solar generators is common to all semiconductors, and may, in fact, be not appreciably worse for silicon than for production cells of gallium arsenide and other materials which had been held out as promising substitutes. The importance of temperature reduction techniques is, therefore, important to all photovoltaic systems, but this investigation is limited to silicon.

The program is divided into three tasks:

- (a) Thermodynamic considerations of cell coatings
- (b) Evaluation of state-of-the-art coatings, and
- (c) Adaptation of the Spectrolab window type coatings to silicon solar cells.

Task (a) involves a brief thermal study of the effect of cell coatings on a typical oriented solar panel. The efficiency gains are determined relative to a similar uncoated panel. The analysis is intended to demonstrate the general usefulness of the technique. To obtain numerical results it is necessary to assume a specific array configuration. For this purpose a typical oriented panel configuration was chosen and all extraneous sources of heat were neglected. The results, therefore, are, in general conservative; for example, for a non-oriented system the effects of the coatings are significantly greater than for the array chosen here.

Task (b) includes the study of spectral characteristics and physical and environmental properties of state-of-the-art coatings suitable for application to silicon solar cells. A survey of all coating firms has been made and coatings have been obtained from two sources other than Spectrolab. Only one of these other coatings was found to be satisfactory. Among the characteristics which are being investigated are the spectral transmittance, reflectance, and emissivity. These parameters are being measured for both coated and uncoated cells. Three types of Spectrolab coatings and one from

Optical Coating Laboratories, Inc., were found to have spectral characteristics suitable for the short wavelength type of cell coating.

This series of four coatings was then further studied in an environmental test sequence approximating those currently in use in various space programs. These specific tests include humidity, high temperature storage, low temperature storage, temperature shock, and vacuum storage. In addition, ultraviolet and beta irradiation tests are being performed.

Task (c) involves the adaptation of the Spectrolab window type coating to silicon solar cells. For this purpose it is necessary to move the I-R reflection band further into the infrared and to provide high transmission efficiency between approximately .5 and 1 micron, as compared with the .4 to .7 micron transmission band of the original coating. Moreover, it is desirable that absorbance in the I-R region beyond 3 microns be introduced so as to increase the emissivity for directly deposited coatings.

Section 2

ABSTRACT

The use of spectrally selective coatings as filters for silicon solar cells is under investigation. The program is oriented primarily toward auxiliary power systems for space vehicles, but the results may, to a certain extent, have other applications. A general study of the thermal balance of a solar panel in space and the resultant effect on array efficiency is examined and a specific example is studied. This example is an isolated, oriented array with an active area utilization of 85 percent. The output of this panel is computed for solar intensities corresponding to Mars, the Earth, and Venus for current coating types and for the "window" type coating currently under study, and the results are compared to a bare panel.

The physical properties and environmental characteristics of state-of-the-art coatings are also being studied. Measurements of the spectral transmittance, reflectance and emittance for coated cells are being obtained. Environmental tests include humidity, high and low temperature storage, temperature shock, vacuum storage and ultra-violet and beta irradiation.

Adaptation of the Spectrolab infrared "window coating" to silicon solar cells is being studied. Three separate problems are under investigation. These include:

1. Modification of the configuration to extend the long wavelength cutoff from 700 to 1000 μ ,
2. Improvement of the environmental stability, and
3. Increase in the long wavelength emissivity.

In connection with the first phase of this task, an experimental curve is presented. In connection with the second and third phases, the rare earth oxides, fluorides and oxyfluorides are under study.

Section 3

PUBLICATIONS, LECTURES, REPORTS AND CONFERENCES

The following publications, lectures, reports and conferences have resulted directly from research and development by Spectrolab under Contract No. DA 36-039 SC-85284 during the period 25 January through 30 June 1960:

Publication and Lecture

"Spectrally Selective Optical Coatings", by A.E. Mann, presented to the Fourteenth Annual Power Sources Conference in Atlantic City, New Jersey, on 17 May 1960 and subsequently published in "Proceedings" by the PSC Publications Committee.

Reports

Monthly Letter of Progress Reports 1 through 6 have been submitted as follows: No. 1, January; No. 2, February; No. 3, March; No. 4, April; No. 5, May; and No. 6, June. All were prepared under the title, "Investigation of Optical Coatings for Solar Cells".

Conferences

Representatives of the Power Sources Division of the U. S. Army Signal Research and Development Laboratory, Fort Monmouth, New Jersey, and of Spectrolab, Incorporated, have met as follows:

In attendance on	George Munrath	Power Sources Div.
23 January 1960 at the	Stuart Shapiro	" " "
Hexagon, Fort Monmouth	Emil Kittl	" " "
16 May 1960 in	William Shorr	" " "
Atlantic City	Alfred E. Mann	Spectrolab
In attendance on	Stuart Shapiro	Power Sources Div.
15 June 1960 at	Alfred E. Mann	Spectrolab
Spectrolab in	Ronald Bell	" "
North Hollywood	Stanley DeCovnick	" "

Section 4

FACTUAL DATA

TASK ONE: Thermal Analysis of Spectrally Selective Cell Coatings

In order to determine the optimum characteristics of spectrally selective coatings for silicon solar cells, it is necessary to obtain the general expression for the efficiency of a coated cell relative to an uncoated one. Since this necessarily involves the thermal degradation of the cell array, the equilibrium temperature must be computed. The thermal balance for a cell in typical application is developed below.

The heat input to a solar array in space is the summation of absorbed direct solar energy, albedo and thermal energy from planets and nearby auxiliary (vehicle) surfaces, internal power losses, and conduction from other portions of the vehicle. The energy output is the summation of thermal radiation to space and nearby surfaces, conduction to other portions of the vehicle, and the converted electrical energy. The equilibrium temperature is that at which the sum of energy input and output is equal to zero, i.e., $Q_I + Q_O = 0$.

Mathematically,

$$\begin{aligned}
 & \int_A \int_0^\infty \alpha(\lambda, \vec{r}, \hat{E} \cdot \hat{n}) (\vec{E}(\lambda) \cdot \hat{n}) dA d\lambda && \text{(Equation 1)} \\
 & + \int_A \int_A \int_0^\infty \alpha(\lambda, \vec{r}, (\vec{r}' - \vec{r}) \cdot \hat{n}) R'(\lambda, \vec{r}', \hat{E} \cdot \hat{n}') (\hat{n}' \cdot \vec{E}(\lambda)) \frac{\hat{n}' \cdot (\vec{r}' - \vec{r}) \hat{n} \cdot (\vec{r}' - \vec{r})}{(\vec{r}' - \vec{r}) \cdot (\vec{r}' - \vec{r})} dA' dA d\lambda && \text{Direct Solar Radiation} \\
 & + \int_A \int_A \int_0^\infty \alpha(\lambda, \vec{r}, (\vec{r}'' - \vec{r}) \cdot \hat{n}) R''(\lambda, \vec{r}'', \hat{E} \cdot \hat{n}'') (\hat{n}'' \cdot \vec{E}(\lambda)) \frac{\hat{n}'' \cdot (\vec{r}'' - \vec{r}) \hat{n} \cdot (\vec{r}'' - \vec{r})}{(\vec{r}'' - \vec{r}) \cdot (\vec{r}'' - \vec{r})} dA'' dA d\lambda && \text{Planet Albedo} \\
 & + \int_A \int_A \int_0^\infty \alpha(\lambda, \vec{r}, (\vec{r}' - \vec{r}) \cdot \hat{n}) \alpha'(\lambda, \vec{r}') \left(\frac{a\lambda^{-5}}{e^{b/\lambda T'} - 1} \right) \frac{\hat{n}' \cdot (\vec{r}' - \vec{r}) \hat{n} \cdot (\vec{r}' - \vec{r})}{(\vec{r}' - \vec{r}) \cdot (\vec{r}' - \vec{r})} && \text{Solar Reflectance from Vehicle} \\
 & && \text{Earth Thermal Radiation}
 \end{aligned}$$

$$+ \int_{\lambda} \int_A \int_0^{\infty} \alpha(\lambda, \vec{r}, (\vec{r}'' - \vec{r}) \cdot \hat{n}) \alpha''(\lambda, \vec{r}'') \left(\frac{a\lambda^{-5}}{e^{b/\lambda T''} - 1} \right) \frac{\hat{n} \cdot (\vec{r}'' - \vec{r}) \hat{n} \cdot (\vec{r}'' - \vec{r})}{(\vec{r}'' - \vec{r}) \cdot (\vec{r}'' - \vec{r})} dA'' dA d\lambda$$

Vehicle Thermal Radiation

$$+ Q_V$$

Internally Generated Heat

$$+ c (T'' - T)$$

Heat Conduction

$$- \int_A \int_0^{\infty} \alpha(\lambda, \vec{r}) \left(\frac{a\lambda^{-5}}{e^{b/\lambda T} - 1} \right) dA d\lambda$$

Solar Array Thermal Radiation

$$- \int_A \int_0^{\infty} \eta(\lambda, T, \vec{E} \cdot \hat{n}) (\vec{E} \cdot \hat{n}) dA d\lambda$$

Solar Converted Energy

$$= 0$$

Where: The unprimed quantities are solar panel elements

The primed quantities are planet elements

The double primed quantities are vehicle elements

A = area of component

\vec{r} = position vector

\hat{n} = unit vector normal to surface at endpoint of the appropriate position vector

C = coefficient of thermal conductivity

η = electrical conversion efficiency

α = spectral absorptivity

T = temperature, °K

R = reflection coefficient

a, b = coefficients, Planck's black body radiation equation

E = solar irradiance

For purposes of this typical analysis, the vehicle position will be considered to be such that there is negligible incident albedo or thermal emission from planets and that the vehicle configuration is such that there is sufficient isolation between the solar array and vehicle to prevent reflectance, thermal emission and conductance to or from the vehicle itself. With these simplifications, and neglecting power losses on the panel, the heat input reduces to direct solar radiation alone. If it is also assumed that the panel temperature is uniform, then the thermal radiation from the panel can be expressed in terms of the more common Stefan-Boltzmann law and the thermal balance equation then simplifies to:

$$\int_{\lambda} \int_A (\alpha)(\vec{E} \cdot \hat{n}) d\lambda dA - \sigma T^4 \frac{\int_{\lambda} \int_A \frac{\alpha \lambda^{-5}}{e^{b/\lambda T} - 1} d\lambda dA}{\int_{\lambda} \int_A \frac{\lambda^{-5}}{e^{b/\lambda T} - 1} d\lambda dA} - (\eta)(E n) d\lambda dA = 0 \quad (2)$$

The integral in the radiative expression of Equation 2 is the effective thermal emissivity, i.e.

$$\epsilon = \frac{\int_{\lambda} \int_A \frac{\alpha \lambda^{-5}}{e^{b/\lambda T} - 1} d\lambda dA}{\int_{\lambda} \int_A \frac{\lambda^{-5}}{e^{b/\lambda T} - 1} d\lambda dA} \quad (3)$$

The above assumptions would correspond for example, to a typical well-designed space probe with an isolated array at a considerable distance from the Earth. In order to obtain some numerical results, such a vehicle will be studied where: the solar panels are flat and perfectly oriented; the active area covers 85% of the front surface, the remaining 15 percent having an emissivity of .2 and a solar absorptivity of .3; the rear surface emissivity is .85; and the nominal cell conversion efficiency is 10 percent*. An analysis of such a system, using Equation 2 with data which will be described below, reveals that the array would reach an equilibrium temperature of 86°C when irradiated by a zero-air-mass insolation of 140 mw/cm.

* Measured at 25°C and air-mass-zero illumination. Such a cell corresponds to a commercial 12% cell (measured under air-mass-one illumination).

This calculation is based upon the zero-air-mass solar irradiance as shown in Figure 4 and the spectral absorptivity (emissivity) for a typical uncoated silicon cell, as shown in Figure 5. For purposes of computation, the emissivity was weighted by the spectral distribution of a 50°C black body as shown in Figure 6.

Using the definition for effective thermal emissivity given in Equation 3 and the geometry and surface characteristics described earlier, the thermal balance (Equation 2) reduces for an oriented panel to:

$$\begin{aligned} E (A_c \bar{\alpha}_c + (1 - A_c) \bar{\alpha}_p - \beta(T)) = \\ c T^4 (A_c \bar{\epsilon}_c + (1 - A_c) \bar{\epsilon}_p + \bar{\epsilon}_r) \end{aligned} \quad (4)$$

where the subscripts c, p, and r, refer to the active cell, inactive panel, and rear panel, respectively; and A_c is the fractional active cell area. For the model panel:

$$\begin{aligned} E &= 140 \text{ mw/cm}^2 \\ c &= 5.67 \times 10^{-12} \text{ watts/cm}^2/\text{deg}^4 \\ A_c &= .85 \\ \bar{\alpha}_p &= .3 \\ \bar{\epsilon}_p &= .2 \\ \bar{\epsilon}_r &= .85 \end{aligned}$$

Using the data of Figures 4, 5, and 6, and performing the indicated product integrals, for a bare cell: $\bar{\alpha}_c = .92$; $\bar{\epsilon}_c = .31$. Substituting this data, Equation 4 may be written:

$$\begin{aligned} .140 (.85 \times .92 + .15 \times .3 - \beta(T)) = \\ 5.67 \times 10^{-12} T^4 (.85 \times .31 + .15 \times .2 + .85) \end{aligned} \quad (5)$$

The cell efficiency β must be adjusted in accordance with the thermal degradation of a typical solar cell (assumed to be operating at maximum power point of the E-I characteristic) as shown in Figure 7. A solution of this implicit equation results in a panel temperature of 86°C and a cell efficiency of 6.7 percent (relative to AMO - 10 percent at 25°C),

It is next desired to determine the effect of application of spectral coatings to the cell surfaces. By evaluating the gains resulting from varying the characteristics of a given class of coatings, it is then possible to determine the optimum specifications for each coating class.

Obviously, the ideal filter would have the highest possible transmission in the energy conversion spectral region, the highest possible reflection in that portion of the solar spectrum where conversion efficiency is negligible, and the highest possible emissivity in the thermal region, beyond 3 to 5 μ . Transitions between reflected and transmitted regions should be quite sharp, but the transition to absorptivity in the 3 to 5 μ region is not critical. Optimization for each given class of filter then reduces to merely determining the proper cutoff wavelength at which the transmission is 50 percent. The analysis was performed by computing the gain effected by varying the cutoff wavelengths and then merely noting the peak of the resulting gain curve.

In computing performance it is necessary to take into consideration the transmission loss of the filter, as well as the efficiency gain resulting from the decreased temperature effected by its presence. The effective transmission factor is given by:

$$\bar{t}_s = \frac{\int_0^{\infty} S(\lambda) E(\lambda) t(\lambda) d\lambda}{\int_0^{\infty} S(\lambda) E(\lambda) d\lambda} \quad (6)$$

where S is the cell sensitivity, E is the solar irradiance, t is the filter spectral transmittance, and \bar{t}_s is the effective transmittance of convertible air-mass-zero insolation, i.e., the relative performance of a coated to an uncoated cell at a given temperature.

The output of the coated panel to the uncoated panel, neglecting second order effects of illumination level on cell efficiency, is simply:

$$\frac{\beta_c}{\beta_o} = \frac{F(T)}{F(T_o)} \cdot \bar{t}_s \quad (7)$$

where F(T) is the functional value of $\beta(T)$ as given in Figure 7. The absolute output per cm² of panel area in 140mw/cm² insolation is:

(8)

$$E \Delta A_c \beta_n \times F(T) \times \bar{\epsilon}_s = .140 \times .85 \times .10 \times F(T) \times \bar{\epsilon}_s = .0119 F(T) \bar{\epsilon}_s \text{ watt/cm}^2$$

where β_n is the nominal cell efficiency at 25°C and zero-air-mass-sun (corresponds to 83% of commercial specification or air-mass-one).

Three different coating types were examined in this study: the Spectrolab ultraviolet rejection filter known as Solakote "A" (typical spectral transmission shown in Figure 8); the blue-violet reflecting filters offered commercially by Spectrolab and OCLI (typical curves shown in Figures 9 and 10 respectively); and an idealized characteristic for the window type coating as shown in Figures 11 and 12. The substrate is assumed to be Corning Type 0211 microsheet glass. The emissivities are, therefore, essentially the same for all the coatings. A typical coated cell emissivity is shown in Figure 13.

The short cutoff of Solakote "A" does not materially affect the solar absorptivity and reduces the effective filter transmission as defined in Equation (5) by less than 2%.

For the blue-violet reflecting filter the effective efficiency gain was computed assuming the spectral characteristics shown in Figure 14, with the cutoff varying from 350 to 550 mμ. Similarly, for the window coating, the characteristics shown in Figures 11 and 12 were used and the short wavelength cutoff was varied over a similar range. The problem arises as to what is the optimum long wavelength cutoff of the window coating for a given short wavelength cuton. This can be determined by consideration of the effects of progressive increments of wavelength on cell performance. The energy in a given wavelength increment produces two effects: It provides an increment of converted energy, and it incrementally heats the cell. The proper match of the long wave cutoff to the short wave cuton is that for which the ratios of converted energy to heating are equal, i.e., if λ_1 and λ_2 are the short and long wavelength transitions, respectively, then:

$$\frac{E(\lambda_1) S(\lambda_1) \Delta \lambda}{E(\lambda_1) \Delta \lambda} = \frac{E(\lambda_2) S(\lambda_2) \Delta \lambda}{E(\lambda_2) \Delta \lambda} \quad (9)$$

This is simply to say that the long wavelength cutoff is that wavelength for which the cell conductivity matches the specific short wavelength cell conductivity, i.e., $S(\lambda_1) = S(\lambda_2)$. The typical cell conductivity curve of Figure 15 was used for determination of the matched point.

The active absorptivity for the coated cell was deduced in each case from measurements of the reflecting absorptance in the ultraviolet. Active reflectivity measurements in the ultraviolet will be obtained shortly and the absorptance will be corrected at that time. Thus, the effective solar energy transmission by the filter is computed by integrating the product \bar{a}_c over the spectrum.

$$\bar{a}_c = \frac{\int \bar{a}_c(\lambda) S(\lambda) d\lambda}{\int S(\lambda) d\lambda} \quad (10)$$

Since the active base cell spectral absorptivity is essentially constant at 92 percent over the solar energy region, for a reflection type coating, assuming reflection of non-transmitted energy, the effective absorptivity for the active cell area can be approximated by:

$$\bar{a}_c = \bar{a}_u \bar{r}_c = .92 \bar{r}_c \quad (11)$$

where the subscripts u and c refer to uncoated and coated cells respectively.

The \bar{a}_c product curves are shown in Figures 16 and 17 for the typical blue-violet reflecting filter (with cutoff at 4.70×10^8 as in Figure 14), and the window coating (as shown in Figures 11 and 12). The results of these integrations and the computations of \bar{a}_c are:

Coating Type	\bar{r}_c	\bar{a}_c
A	.85	.92
B	.78	.72
C	.59	.54

Substituting these results into Equation 5, the equilibrium temperature is shown in Figure 18 as a function of rear surface emissivity for the three coating types and a bare panel. In Figure 19, the rear surface emissivity has been set at .85 and the illumination level is varied.

The output of the resultant coated panel relative to an uncoated panel for the above model is obtained from Equation 7 using the above data. The results are plotted in Figure 20 for the three coating types under illumination levels corresponding to orbits near Venus, the Earth and Mars. As would be expected, the higher selectivity is desired for the higher illumination levels. Thus, near Venus, the window type coating more than doubles the panel output of the bare cell. Near Earth, the window type coating is also very effective in providing a gain of approximately 40%. At the low illumination level near Mars, the increased selectivity of the window coating is of questionable value, and for economic reasons would not be recommended.

The optimum cutoff wavelengths for the various coating types for each illumination level are those for which the relative output curves peak. Actually, the coating specifications are dependent upon the solar panel characteristics and the orbital conditions. The results plotted in Figure 20 and the conclusions which follow are for the model panel described on Page 8. Under illumination conditions near Mars, the use of any coating must be justified by other considerations than increased efficiency, i.e., mechanical erosion or damage from micrometeorites or beta radiation, etc. Near Earth the effects of the coatings are significant and near Venus the coatings should be as selective as possible.

For the blue-violet reflecting filter on an Earth satellite, the optimum cuton wavelength would be between 400 and 450m μ . The output is, however, not appreciably greater than for Solakote "A" with a 400 m μ cuton. Near Venus, the optimum cuton wavelength for the blue-violet reflection filter would be approximately 450 m μ . The output would be almost twice that for an uncoated panel.

For the model panel in an earth orbit, the equilibrium temperature with a window coating with a 350/1130 bandpass would be approximately 25°C. As the bandpass is narrowed and the reflection increased, the temperature declines to -11°C. for a 500/980 bandpass. Referring to Figure 7, it is seen that the slope of the efficiency versus temperature curve begins to decline appreciably below 0°C. so that no significant advantage arises from the greater selectivity of the narrower bandpass.

Near Venus the optimum bandpass for the window coating would have 50% points at 450 and 1050 μ . For the model panel, the output would be approximately 2.25 times that of the uncoated panel (35% higher than for the Solakote "A" panel).

The assumed characteristics for the model panel would generally result in lower temperatures than for other configurations and environments. For example, incidence of planet albedo and IR would raise all temperatures. The effect of higher temperatures would be to increase the efficiency gains arising from the coatings. The greatest differences would be seen in all curves for a Mars orbit and for "Solakote D" in an Earth orbit. The window coating would achieve greater relative gains and the output characteristic as shown in Figure 20 would be modified to introduce peaks more like those for the Venus illumination level.

Summarizing the above data and conclusions, for solar cells with the response and thermal characteristics of Figures 15 and 7, an appropriate wavelength cuton specification for both the blue-violet reflecting and the window coating would appear to be approximately 450 μ , for illumination levels corresponding to the Earth through Venus. Near Earth, all three coating classifications provide significant power gains, but the ultimate choice will depend upon a careful thermal analysis for each vehicle configuration. The window coating will be considerably more important for some panel configurations than for the model investigated here.

For higher illumination levels, the greater selectivity of the window coatings is of great importance. For levels corresponding to Venus ($268\text{mw}/\text{cm}^2$), the long wavelength cutoff should be about 1050 μ .

For systems using optical concentration, a window coating with still greater selectivity may be necessary. However since this program does not include consideration of such devices, no analysis has been included in this report.

TASK TWO: Evaluation of State-of-the-Art Coatings

A survey was conducted by mail of all manufacturers of vacuum deposited coatings and solar cells to solicit their cooperation in this phase of the effort. The Fish-Schurman Corporation and Optical Coating Laboratories, Inc. indicated a willingness to cooperate. Replies from Eastman Kodak and Baird-Atomic indicated that they are not at the present time offering coatings specifically for solar cells. We were informed by personal contact of Bausch and Lomb's willingness to cooperate, but no formal acknowledgement has been received from them.

This program has, therefore, proceeded using the following coatings:

1. Spectrolab Type A-42	Figure 21
2. Spectrolab Type B 1/5/460	" 22
3. Spectrolab Type B 2/0/470	" 23
4. OCIL Type 207 SOI 460	" 24
5. Fish-Schurman Type 3119	" 25

The evaluation consists of the following phases:

- (a) Measurement of Spectral Characteristics
- (b) Evaluation of Suitability for Application to Silicon Solar Cells
- (c) Testing of Environmental Stability

PHASE (a): Measurement of Spectral Characteristics

Samples of the above filters were laminated to a .040" glass plate of index 1.52 and the transmittance curves measured over the region .3 to 1 micron on a Perkin-Elmer Spectracord monochromator. The results are presented as Figures 21 through 25. In Figure 26, is the published typical curve of the Fish-Schurman filter. The transmissions have been raised by 4-1/4% to account for the second surface reflectance of the mounting plate. The curves are, therefore, representative of the filter, as applied to the solar cell.

The Fish-Schurman filter has an effective transmission loss of more than 10%. Although this configuration does have a narrow reflection in the near I-R, the gain resulting from the thermal effects would not balance the filter transmission loss. Moreover, this sample is characterized by a significant ultraviolet-violet spectral "leak" which would not protect against UV degradation of bonding resins. For these reasons, no further investigation was made of the Fish-Schurman Type 3119 filter.

The remaining four coatings are under continuing investigation. Any other coatings which become available will also be evaluated as time permits. The OCLI Type 207-SOC is spectrally equivalent to Spectrolab B/2/C. The Spectrolab B/1/S coating has somewhat higher ultraviolet reflectance, and hence is slightly more efficient as a spectrally selective coating, but is somewhat sensitive to humidity. On the other hand, it is not as sensitive to cold temperature extremes and holds up well at temperatures of below -130°C .

The infrared reflectances of three typical cells coated with various glass type coatings are shown in Figures 27, 28 and 29. This data was obtained on a Perkin-Elmer Model 13 Spectrophotometer with specular reflectance attachment. Since there is very little scattering from the surfaces, the specular reflectance adequately describes the structure of the filter infrared characteristics.

The ultraviolet reflectances of the various filters are currently under investigation and data will be presented in the next report.

PHASE (b) Evaluation of Suitability for Application to Silicon Solar Cells

The five coatings investigated to date are all of the glass type. Some directly deposited coatings will be examined later. The three Spectrolab coatings were deposited on 3 mil Corning microsheet glass, Type 0-211. The OCLI coating was deposited on 6 mil Corning 0-211 microsheet. The Fish-Schurman coating was deposited on an unknown .040" thick glass.

Except for use in high radiation fields, it is generally desirable to keep the glass as thin as possible. For this reason, many contractors specify 3 mil slips, although 6 mil slips are also widely used. In applications where radiation damage is anticipated, special radiation resistant glasses of the order of .060" to .070" may be required. The substrate supplied by Fish-Schurman is considered unsuitable, but no attempt was made to obtain thin slips from them, since the spectral characteristics of the coating supplied did not meet the general requirements for the application.

There appeared to be no particular difference in handling of the other coatings and, aside from the humidity question on the Type B1/S coating, they are all considered suitable for application to cells.

PHASE (c) Testing of Environmental Stability

The four coating types (1 through 4 above) which were approved for spectral characteristics were included in an environmental test series. In evaluating environmental capabilities, it is necessary to examine also the bonding resins, since the characteristics are interdependent. All transparent resins known to be suitable for bonding glass slips to solar cells are being included in the evaluation. The following group of resins was selected for the first test series:

- a. Spectrolab Type E-40
- b. Spectrolab Type E-60
- c. Spectrolab Type E-61
- d. Spectrolab Type E-65
- e. Biggs Type R 823
- f. Biggs Type R 313
- g. Dow Corning Type Q 3-0040
- h. Furane Type 15E
- i. Furane Type 212
- j. Marblette Type 655

Spectrolab Type E-40 was not included in the investigation. This resin is a new formulation which unfortunately, did not progress to a point where it could be included in the original series.

Environmental tests were performed on three different test sample configurations. For ultraviolet irradiation, three slips are mounted on 2"x2"x.040" glass backing plates. For beta irradiation, the coatings are applied directly to Corning type 7940 quartz, half of which are laminated to a second quartz plate (the other half are not). The third test sample configuration, used for all other tests, consists of twenty cells assembled into four 5-cell shingles which are mounted on aluminum plates. All combinations of the nine resins and four coatings are included in the tests, making 36 configurations in all.

The following environmental tests which are known to be pertinent and of concern for coatings have been included in this program. Tests such as vibration which are not of concern for coatings have not been included. The tests have been designed to conform with the general level required for most satellite missions. In some cases, the severest of such test conditions have been used. Following is a summary of the various environmental exposures:

1. Humidity

The samples are placed in a thermostatically controlled Benec humidity chamber operating at a constant level of greater than 95% relative humidity at 55° C. The samples are removed after 50 hours and dried, cleaned, inspected and photographed.

2. High Temperature Storage

The samples are placed in a Thelco pre-heated thermostatically controlled oven set at 80°C. The temperature of a typical plate reaches 78°C in less than 1 minute. Samples remain in the oven for 12 hours and are then removed, cleaned, inspected and photographed.

3. Low Temperature Storage

The samples are placed in a pre-cooled thermostatically controlled environmental chamber, whose temperature is lowered to -75°C in 5 minutes. A typical sample plate reaches -73°C approximately one minute after the chamber. The samples are maintained at this temperature for 12 hours, after which time they are removed, cleaned, inspected and photographed.

4. Temperature Shock

The samples are placed in a specially constructed cold chamber and the chamber is reduced to -75°C in less than 2 minutes. This temperature is maintained for 15 minutes. The chamber temperature is then raised to +25°C in 2 minutes, maintained at 25°C for 15 minutes and lowered to -75°C in 2 minutes. Ten complete cycles are performed. On completion of the final cycle, the samples are returned to room temperature, removed, cleaned, inspected and photographed.

5. Vacuum Storage

The samples are placed in a vacuum chamber which is evacuated in 10 minutes to a pressure of 10^{-5} mm of mercury. The sample is stored in

this vacuum at room temperature for 6 hours, and is then removed, cleaned, inspected and photographed. The test is then repeated with the sample maintained at a temperature of 65°C.

6. Ultraviolet Irradiation

The special samples prepared for the ultraviolet irradiation tests are exposed for a period of 6 hours to a source having an ultraviolet irradiation equivalent to 1500 times the air-mass-zero sun. In a period of 6 hours it is thus possible to simulate the integrated effect of the sun for a one-year orbit with 100% illumination. For non-oriented satellites and those which pass into the Earth's shadow, this would be equivalent to as much as 4 to 6 years of irradiation.

The early tests are being performed in an air atmosphere. The effect of an air environment for such tests is to accelerate damage. However, since the resins are covered except for a thin glue line at the boundaries, the tests in air should be equivalent to those in vacuum. The illuminated area extends across part of the cell edges. If any damage is noted at these points, additional testing in vacuum will be performed.

The test source consists of a GE Mercury AH 6 lamp in a water cooled quartz jacket focused by means of a two-lens quartz aspheric combination so as to illuminate an area approximately 25 x 1.5 mm. A schematic diagram and a photograph of this apparatus are shown in Figures 30 and 31.

7. Beta Irradiation

The special samples prepared for beta tests will be irradiated with a current density of $1.6 \mu\text{a}/\text{cm}^2$ at an energy level of 750 kev. At this irradiance, in one second, 10^{13} electrons/ cm^2 would be incident. Integrated test durations will be 10 and 100 seconds, corresponding to 10^{14} and 10^{15} electrons/ cm^2 , respectively. The spectral transmission of the samples will be measured before and immediately after irradiation.

8. Future Tests to be Included

- a. Very high vacuum, to pressures less than 10^{-5} .
- b. Vacuum testing of resin samples (without coatings).
- c. Temperature cycling -120°C to +80°C to -120°C etc. for a minimum of 30 cycles with transitions occurring in less than 5 minutes and constant temperatures maintained for at least 30 minutes.
- d. Ultraviolet irradiation in vacuum.

9. Test Conclusions to Date

The results for the five-test series completed to date are included as Tables I through V. The filter failures are described as severe, moderate, light and cracked glass. A small glass crack arising generally from thermal stresses in the cold test is not considered serious. A light filter failure represents a difficulty which is barely noticeable under careful examination, but is not generally noticeable to an unskilled inspector. A moderate failure is clearly noticeable and would be cause for rejection at Spectrolab, but unless it were to become more severe, would not degrade module performance. A severe failure is one which covers at least 10 percent of the cell area. The demarkation between moderate and severe damage is to a certain extent subjective.

For the above test series no failures were encountered for any combinations in either the hot or vacuum tests. Between half and all of the filters bonded with resins e, f, g, i and j failed in humidity for all types. As expected, coating type 2 failed in humidity in varying degrees for the remaining four resins b, c, d and h. Spectrolab resin type E-65 in combination with coating types 1, 3 and 4 appears most suitable. For this resin, aside from a small filter crack for coating type 3, only one moderate failure was encountered for filter type 4. Samples using resin types b, c and h were characterized by a scattering of moderate and light failures and filter cracking. By slightly modified compounding, more careful handling or for somewhat less severe environmental tests, these three resins may meet the requirements for this application, and they will therefore be examined in further detail as time permits.

When used with the proper resins, coating types 1, 3 and 4 are all found to meet the general environmental requirements for this application. The numbers of test samples (20 each) were insufficient for fully establishing environmental capabilities, and it is suggested that further testing be made in connection with specific vehicle programs.

Mr. Marshal Pearlman has been investigating additional resins and has prepared a further group which may be included in these tests if time permits.

TASK THREE: Adaptation of Window Coatings to Solar Cells.

Particularly for higher illumination levels, the ideal solar cell coating has a transmission window extending roughly from $.45$ to 1.04μ , reflecting the regions below and above (to about 3μ) this band, and providing high absorbance in the region beyond 4 or 5μ .

Several different coating techniques could conceivably be used to achieve the basic window selectivity. These might include certain semi-conducting films, such as metallic sub-oxides, e.g. stannous oxide, etc., doped with appropriate impurities to induce metallic reflection properties in the near infra-red, while preserving high transmission properties in the visible. By combining such a film with a short wavelength multilayer reflector and a long wavelength absorbing medium, the desired properties could be achieved. However, theoretical considerations lead to the conclusion that to achieve sufficiently high reflectance in the near infra-red, the absorption loss in the visible would exceed 10 percent. Experimentally this conclusion has been borne out in programs aimed at providing visible-transmitting infra-red reflectors and electrically conducting films. Moreover the transition from transmission to reflection for such coatings is rather gradual, whereas sharp demarkation between the regions is important.

The most direct solution to the problem would be through use of a multilayer interference filter. However, to be effective, such a filter must reflect the region from just beyond 1 to at least 2μ . By normal interference methods, a constructive interference band formed of alternating layers all having optical thicknesses nt would produce a primary reflection band at a wavelength of $4 nt$. Additional reflectance bands would be formed at wavelengths of $4/3 nt$, $4/5 nt$, etc. Actually, because of dispersion these additional bands are peaked at somewhat longer wavelengths. Thus, with a quarter wave reflection band at 1.5μ , there would be a three-quarter wave band at $.5 \mu$, an intolerable situation.

On the other hand, the width of the reflection band is proportional to its peak wavelength and inversely proportional to its order. Thus the three-quarter wave band has approximately $1/9$ the bandwidth of the

quarter wave band. For a conventional multilayer interference filter composed of alternating dielectric layers, the bandwidth depends upon the index ratio of the two materials. Suitable materials with visible transparency are limited to such high index materials as zinc sulfide, cerium dioxide and titanium dioxide, etc. (with indexes of the order of 2.3 to 2.6 in the visible and 2.2 to 2.45 in the near infra-red), and to such low index materials as cryolite, chiolite and magnesium fluoride (with indexes ranging from approximately 1.3 to 1.4). There are, of course, numerous intermediate materials which may also be given consideration for such special properties as long wavelength emissivity.

With such materials as those mentioned above, a rough rule of thumb is that the first order reflection band covers the band from roughly 82 percent to 122 percent of the center wavelength. Thus, a reflection band at 1.5μ would have a bandwidth of 600μ , extending approximately from 1.23 to 1.83 . The three-quarter wave peak would fall at about $540 \text{ m}\mu$ (shifted from $500 \text{ m}\mu$ due to dispersion) and would have a bandwidth of approximately $65 \text{ m}\mu$. Shortening the coating so that the cut-off falls at approximately 1.05μ , the 50 percent band limit would fall at about 1.56μ and the three-quarter wave band would cover between 420 and $480 \text{ m}\mu$. This in effect has been done for the Fish-Schurman cell coating, type 3119. It should be pointed out, however, that such coatings generally have excessive transmission losses in the actinic region and the reflection bandwidth, which is only about $500 \text{ m}\mu$ in the near infra-red, is insufficient for cell coating. Examples of such coatings are shown in Figures 25 and 33.

Realizing the difficulty of this task, it was immediately decided to adapt an unusual filter configuration which has been explored at Spectrolab. This coating differs from the conventional reflection stack. A sample of such a reflection filter is shown in Figure 34. Note that there is no secondary three-quarter wave reflection band as in the conventional interference filter. Adaptation of this filter to the solar cell application requires the following tasks:

First, the spectral characteristics needed to be modified by addition of a conventional short wave band filter to form a band covering the range from 1.05 to 1.6 μ .

Second, this filter is known to be somewhat unstable (particularly under prolonged exposure to elevated temperatures) and hence the material structure must be modified to improve stability.

Third, it is desirable to introduce into the filter materials which have high emissivity in the region beyond 4 microns. Such absorbing materials would make possible direct deposition.

The last two problems reduce to a material survey. To improve stability, suitable interlayer films which will reduce diffusion and chemical reaction are desired. To improve infra-red emissivity, these protective films should have high infra-red absorbance. The infra-red properties of a number of materials are therefore being investigated. These include the rare earth oxides, oxyfluorides and fluorides which have good thermodynamic stability and which should control diffusion. The intermediate infra-red properties are being studied. A literature search failed to locate any pertinent data beyond 2 μ , although some information has been published by Hass, et al, for the shorter wavelength regions. Some of this data is presented in Figure 35 which shows the refractive indexes of oxides and fluorides of lanthanum, praseodymium and neodymium.

As an alternative, silicon monoxide or silicon dioxide could be used, but there is still some concern about their stability in the high radiation and ultraviolet fields of near Earth space.

This portion of the program has been delayed considerably by problems associated with the move to our new laboratory. Unfortunately this move is some ninety days behind schedule. Equipment which was ordered for carrying out the special evaporation experiments is now

ready for installation and will be coordinated with the completion of that portion of our new laboratory during the next few weeks. Unfortunately these delays, which were beyond our control, have seriously impeded progress in this phase of the program.

Attempts to evaporate the above listed rare earth materials in our present evaporation plants proved unsuccessful. All films were soft and opalescent. It was therefore decided to postpone any major emphasis on this task until suitable equipment became available.

Realizing, of course, the physical limitations, several samples of the early Spectrolab window coating have nevertheless been produced. Combining this coating with a short wavelength reflector, the resultant transmission curve is shown in Figure 36. Note that this characteristic closely approximates the desired window properties as expressed in the original goal of the program as indicated in Figures 11 and 12. These coatings will be repeated on thin slips for application to cells and some temperature equilibrium studies will then be performed.

In the meantime it is hoped that additional progress on the material study will be effected so that satisfactory physical characteristics can also be achieved.

Section 5 CONCLUSIONS

The program has been divided into three separate tasks. The first task includes a theoretical evaluation of the thermal gains from solar cell coatings. Several different filter and array configurations have been examined and the results are presented. In this report, a specific array was chosen which is described in Section 3, Task One. For this particular model array in an Earth orbit, a gain of as much as 40 percent in cell efficiency can be expected, and for a Venus orbit, an increase by a factor of more than 2. For other array configurations (for example, a non-oriented system) the gains will be even greater, and for concentrator systems the coatings are of even more significance.

In Task Two state-of-the-art coatings are evaluated. For general purpose applications, the only approved coatings appear to be Spectrolab's type A and B/2 and the Optical Coating Laboratories' type 207 SCC. All three coatings yield approximately equivalent efficiency gains and are found to be environmentally stable when used with a limited group of resins. The resins so far found to be promising include Spectrolab's types E-60, E-61, and E-65 and Furane's type 15 E.

The evaporation program has been delayed significantly by equipment and facility problems associated with our move to new quarters. Some limited evaporations have been completed and a sample having approximately the desired spectral properties has been prepared. The sample transmission characteristics are shown in Figure 36.

Efforts will continue, particularly on the Third Task and to a certain extent on the Second Task of the program.

Section 6
PROGRAM FOR THE NEXT INTERVAL

The present move to our new laboratory and momentary arrival of considerably expanded facilities should permit an increased effort and productivity during the next period. The key to the success of this program lies in the material study for antidiffusion films for the Spectrolab window coating.

During the next period emphasis will be shifted to work on preparation of improved window films. In particular, the efforts will be concentrated on the above-mentioned materials study and on an experimental determination of equilibrium temperatures of coated cells, particularly with the experimental window coatings prepared to date and those which will be prepared during the next few weeks.

As soon as materials having suitable optical properties are developed, they will be introduced into the coatings in an attempt to improve the near infra-red emittance. Efforts will continue with the present material complex to study the effects of impurities and methods of film preparation on coating stability.

Discussions with Dr. Hass have indicated that their results for rare Earth salts were obtained by very fast evaporations from enclosed boats. Our attempts to evaporate from filamentary heated crucibles were found unsatisfactory and hence the enclosed boat method will be tried in the new evaporators. Secondly, heavy out-gassing of the materials prevented maintenance of a suitable vacuum for preparation of physically suitable films.

A small amount of effort will be required for the state-of-the-art coating evaluation task, particularly to complete the ultraviolet and beta irradiation experiments. In addition, a survey series of suitable resins has been completed by Mr. Marshal Pearlman. These new resins are presently being prepared and will be evaluated as time permits.

Section 7
IDENTIFICATION OF KEY PERSONNEL

The work described in this report has been and will be performed by and under the guidance of the following Spectrolab personnel:

Alfred E. Mann, President

Mr. Mann is a graduate of the University of California at Los Angeles with extensive graduate work in nuclear and mathematical physics. He has completed the academic studies and oral examinations for the Ph.D. degree and is a member of Pi Mu Epsilon and Phi Beta Kappa honorary societies. He is active in various professional societies, including the Optical Society of America, the American Rocket Society, the Spectroscopy Society, the American Chemical Society, the Coblenz Society, and the Society of Motion Picture and Television Engineers.

Mr. Mann, for five years President and Director of Engineering of Spectrolab, has contributed significantly to advances in radiometry, vacuum physics, thin-film optics, and advanced methods of mathematical analysis. He has patented two inventions, and five more patents are pending. Formerly Mr. Mann was a project supervisor at the Technicolor Corporation, where he directed research in the fields of radiation damage, optical physics, radiometric instrumentation, and digital and analog computer programming.

Author of many scientific papers, Mr. Mann's publications during this past year include "Spectrally Selective Optical Coatings for Solar Cells", "Design Considerations for Solar Simulation", "Solar Panel Design Considerations", and "Narrow Band Filters for Emission Spectroscopy", presented at the Power Sources Conference, the American Rocket Society Space Power Systems Conference, and the Pittsburgh Conference on Analytical Chemistry.

Dr. Ronald Bell, Senior Physicist

Dr. Bell graduated with first class honors from the Royal College of Science in London with majors in special math and special physics. He is a member of the Institute of Physics, British Institute of Radio Engineers, British Institute of Electronic Engineers, and the American Physical Society. His employment experience includes positions with the British Telecommunications Research Establishment, De Havilland Propellor Company, Technicrystals, Westrex Corporation, Universal Transistor Products, and Greer Hydraulics (Director of Research). Dr. Bell is now employed as a Senior Physicist for Spectrolab.

Virginia Larsen, Physicist

Mrs. Larsen graduated from the University of Southern California and obtained her MA at Los Angeles State College. She has eight years' experience in the fields of infra-red, ultraviolet, and mass spectroscopy; having been engaged as a physicist and chemical engineer with the Shell Oil Company, as an instructor in physics, engineering, and astronomy at Long Beach City College; and is a lecturer in astronomy at the University of California at Los Angeles. A master's degree in astrophysics with a specialty in meteorites is pending from U.C.L.A. Mrs. Larsen is currently employed as a physicist by Spectrolab.

Approximately 1700 hours have been expended on this project during the period 25 January 1960 through 30 June 1960:

Alfred E. Mann, Senior Physicist	220 hours
Ronald Bell, Senior Physicist	90 hours
Virginia Larsen, Physicist	400 hours
technicians	990 hours

TEST NO. 1
HUMIDITY TEST RESULTS

(Numbers in parentheses refer to number of glass cracks)

Failures	Filter Type 1				Filter Type 2				Filter Type 3				Filter Type 4				
	RESIN	Severe	Moderate	Light	TOTAL	Severe	Moderate	Light	TOTAL	Severe	Moderate	Light	TOTAL	Severe	Moderate	Light	TOTAL
A																	
B				0		0		0				(2)					0
C			5	5	20				20			4	4				0
D				0	20				20				0				0
E	13	2		20					0		15		15	15	5		20
F		9		9	9				9		10		10		13		13
G	13	4		17	20				20	20			20	5	4		9
H				0	20				20				0		1		1
I	20			20	20				20	20			20		16		16
J		13		13	20				20				(13)	12			12

TEST NO. 11
HIGH TEMPERATURE TEST RESULTS

RESIN	Filter ₁ Type				Filter ₂ Type				Filter ₃ Type				Filter ₄ Type			
	Severe	Moderate	Light	TOTAL	Severe	Moderate	Light	TOTAL	Severe	Moderate	Light	TOTAL	Severe	Moderate	Light	TOTAL
A																
B				0				0				0				0
C				0				0				0				0
D				0				0				0				0
E				0				0				0				0
F				0				0				0				0
G				0				0				0				0
H				0				0				0				0
I				0				0				0				0
J				0				0				0				0

LOW TEMPERATURE TEST RESULTS

(Numbers in parentheses refer to number of glass cracks)

Failures	Filter Type 1				Filter Type 2				Filter Type 3				Filter Type 4				
	RESIN	Severe	Moderate	Light	TOTAL	Severe	Moderate	Light	TOTAL	Severe	Moderate	Light	TOTAL	Severe	Moderate	Light	TOTAL
A																	
B			2		2	16			16				(2)		2		2
C			3		3				0				(7)			1	(2)
D					0				0				(1)		1		1
E					0				0		6		6 (4)				(1)
F			6		6 (1)				0				(9)				(5)
G					0				0				0				0
H					(3)				0				(6)				(2)
I					0				0				0		3		3
J			3		3				0	10			10		4		4

TEST NO. IV

TEMPERATURE CYCLE TEST RESULTS

(Numbers in parentheses refer to number of glass cracks)

Failures	Filter Type 1				Filter Type 2				Filter Type 3				Filter Type 4			
	Severe	Moderate	Light	TOTAL	Severe	Moderate	Light	TOTAL	Severe	Moderate	Light	TOTAL	Severe	Moderate	Light	TOTAL
A																
B		1		1				0				0		4		4 (2)
C				0				0				0				0
D				0				0				0		3		3
E				0				0				0		3		3
F				0				0				0				0
G				0				0				0				0
H				0				0				0		1		1
I				0				0				0		1		1
J		4		4				0		2		2		3		3

TEST NO. V.
VACUUM TEST RESULTS

Failure	Filter Type 1				Filter Type 2				Filter Type 3				Filter Type 4				
	RESIN	Severe	Moderate	Light	TOTAL	Severe	Moderate	Light	TOTAL	Severe	Moderate	Light	TOTAL	Severe	Moderate	Light	TOTAL
A																	
B				0	0				0				0				0
C				0	0				0				0				0
D				0	0				0				0				0
E				0	0				0				0				0
F				0	0				0				0				0
G				0	0				0				0				0
H				0	0				0				0				0
I				0	0				0				0				0
J				0	0				0				0				0

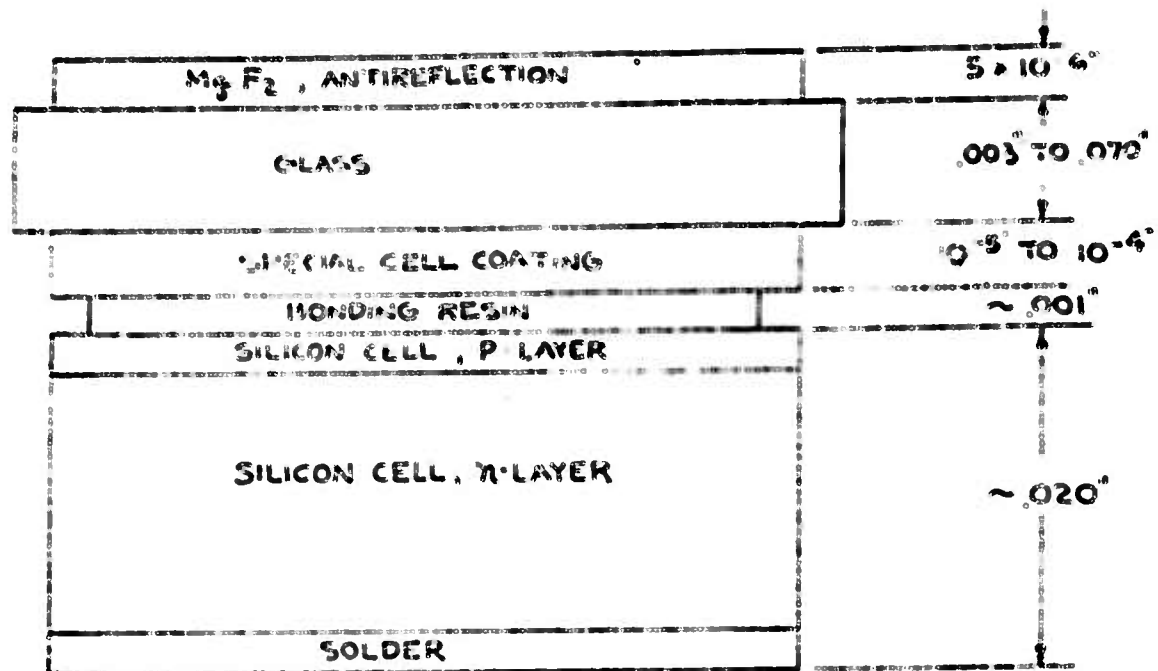


FIGURE 1
 SCHEMATIC OF COATED SILICON CELL,
 GLASS TYPE COATING

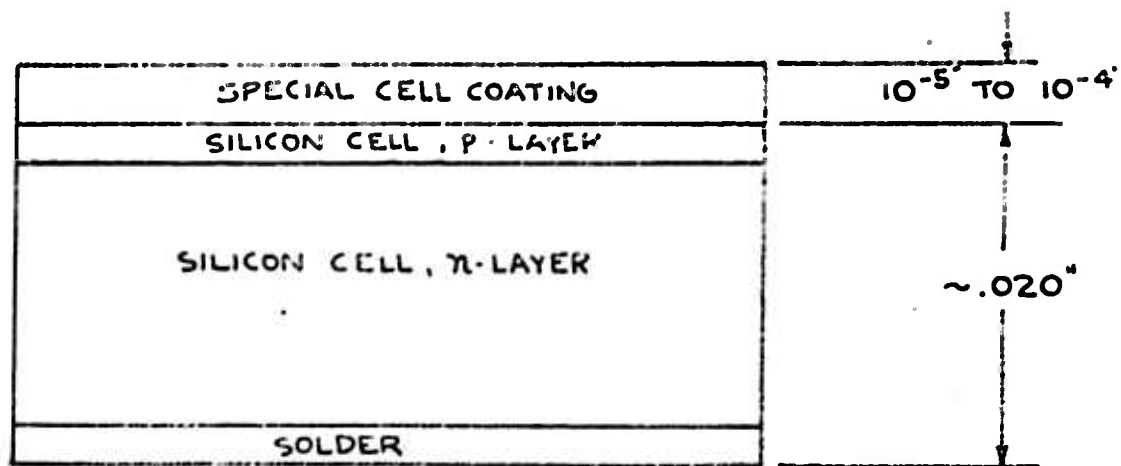


FIGURE 2
 SCHEMATIC OF COATED SILICON CELL,
 DIRECT COATING.

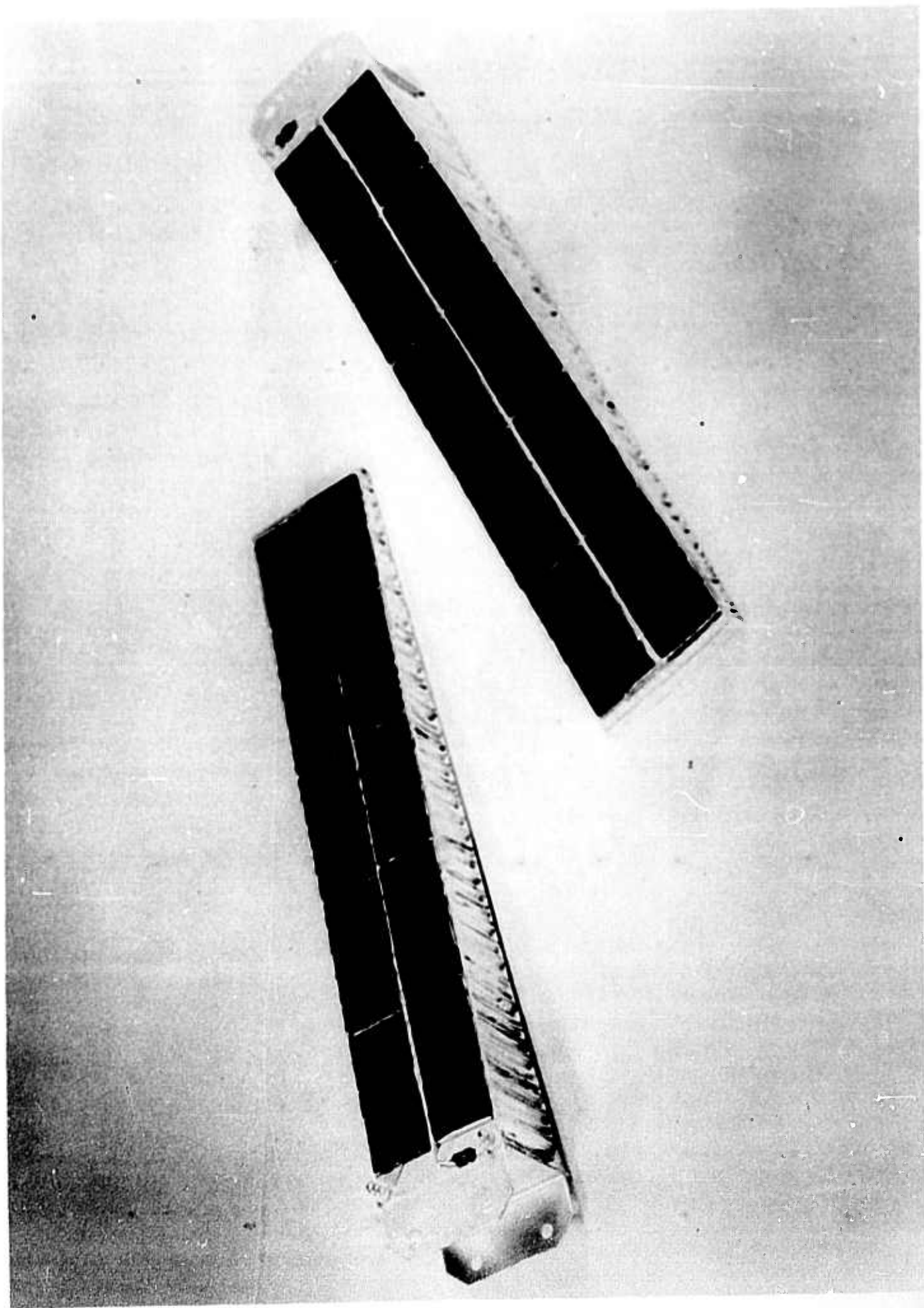


Figure 3. Typical Coated Solar Cell Modules (Explorer VI and Pioneer V)

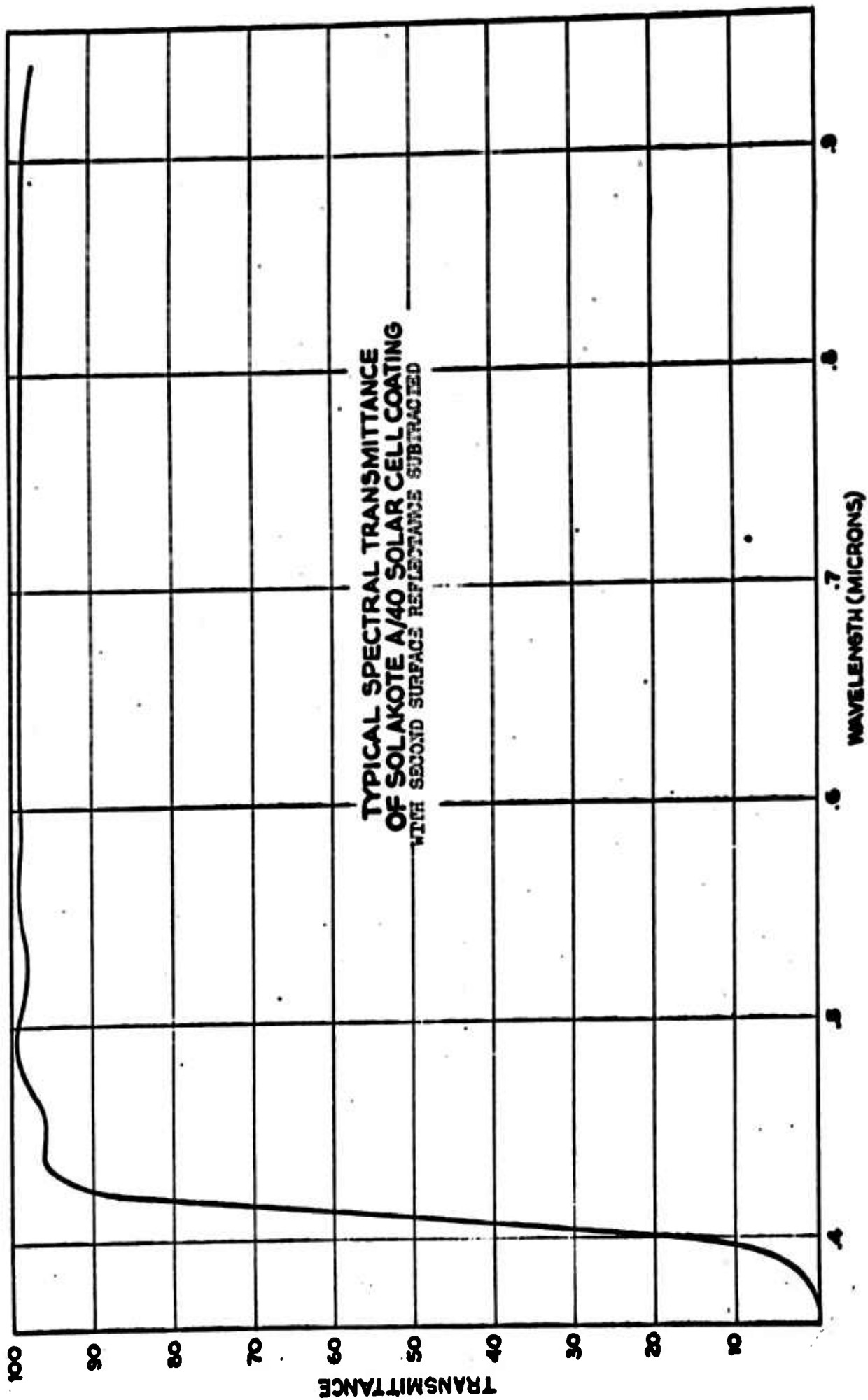
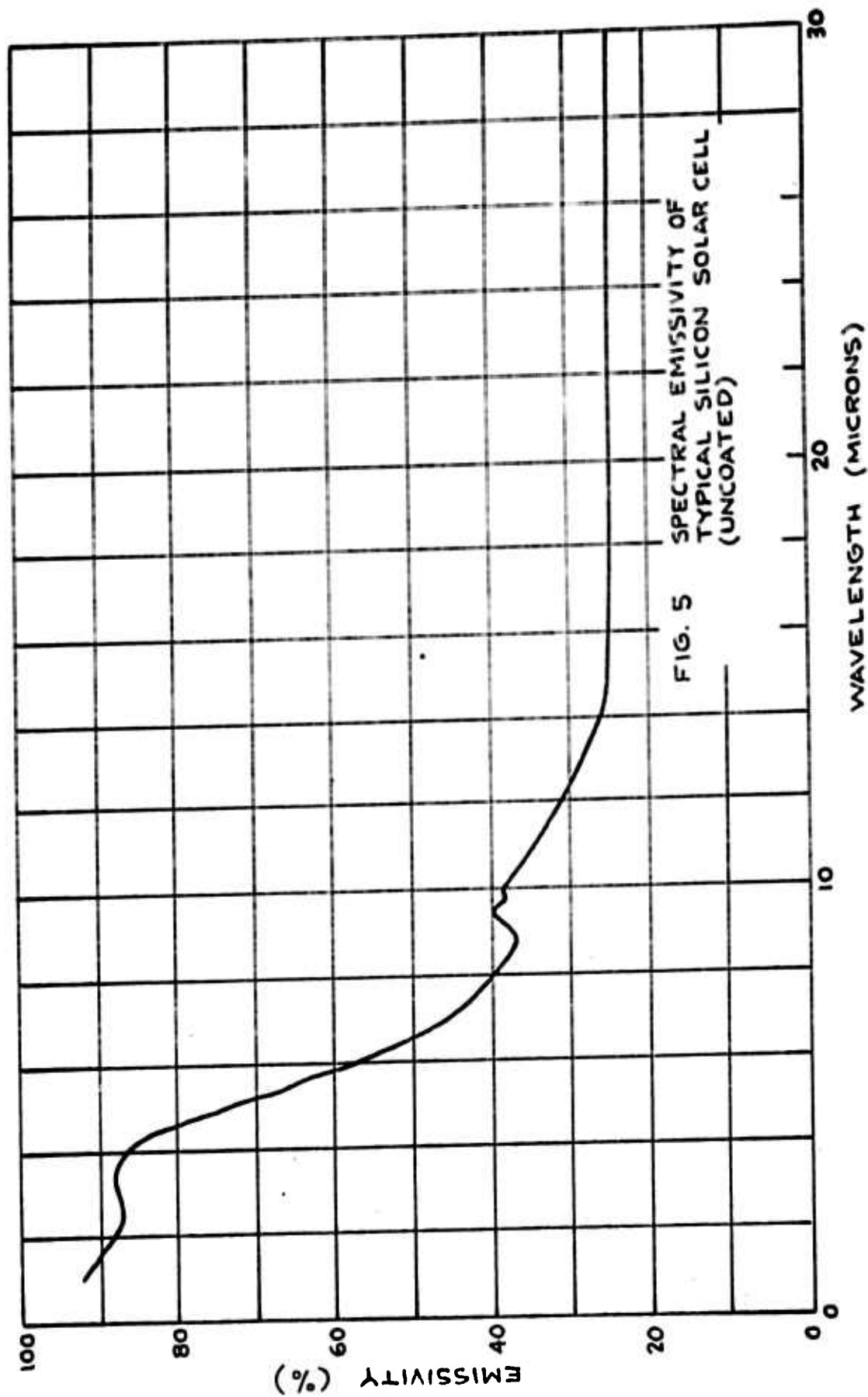


FIG. 4



**SPECTRAL EMISSIVITY FOR BLACK BODIES
AT 50°C.**

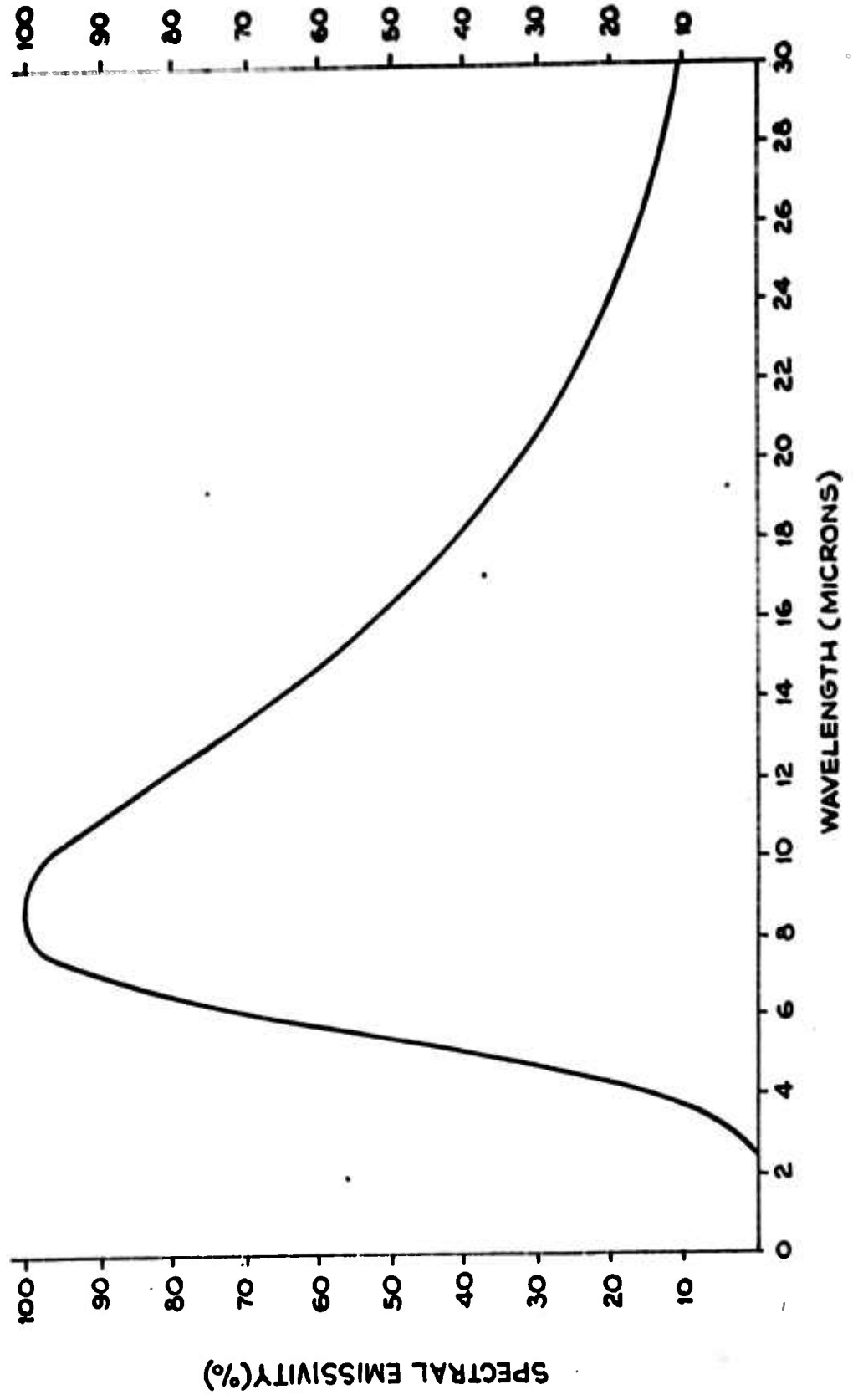


FIG. 6

RELATIVE THERMAL EFFECTSON
MAXIMUM POWER FOR TYPICAL
SILICON SOLAR CELL

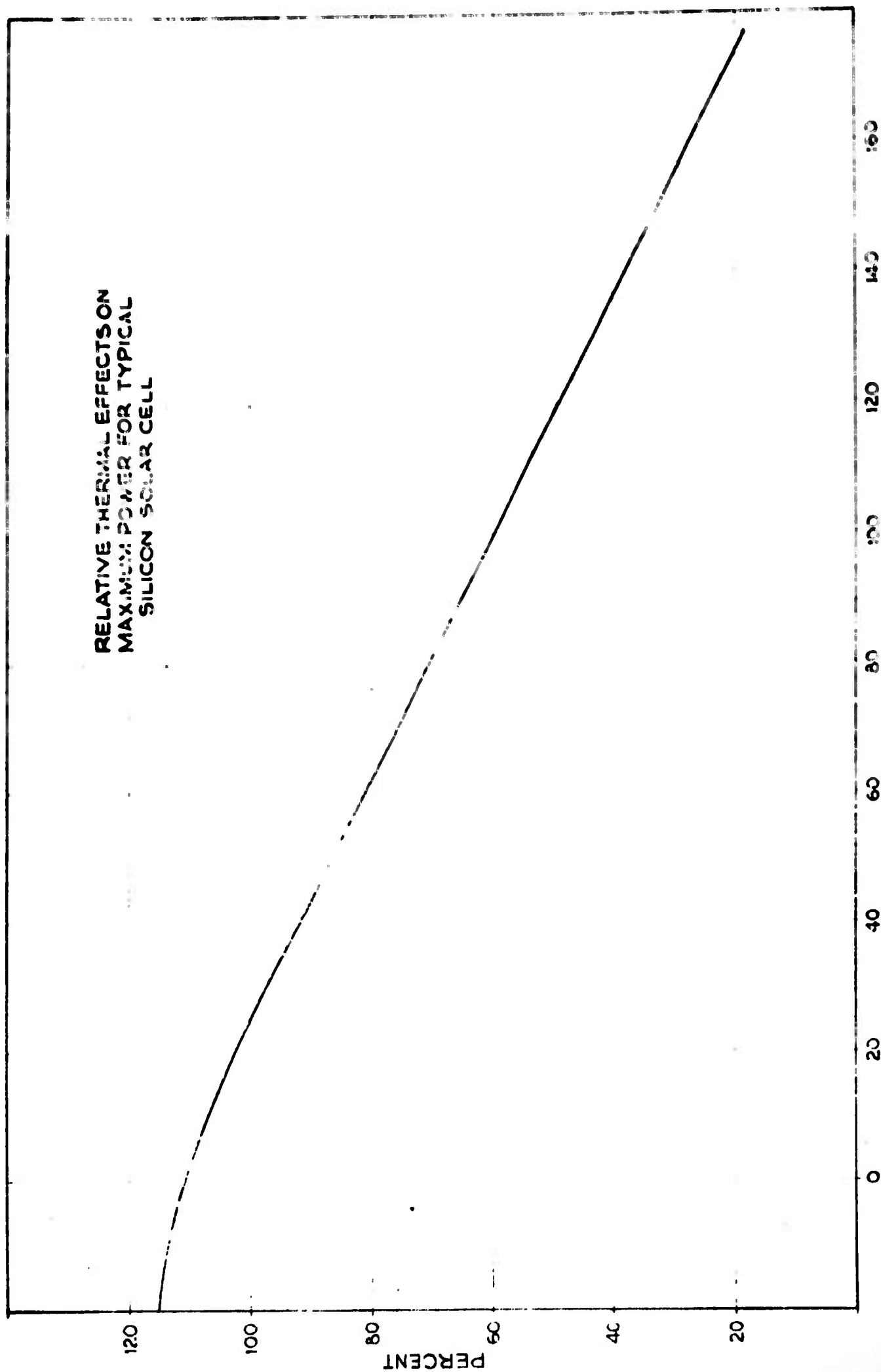


FIG.7

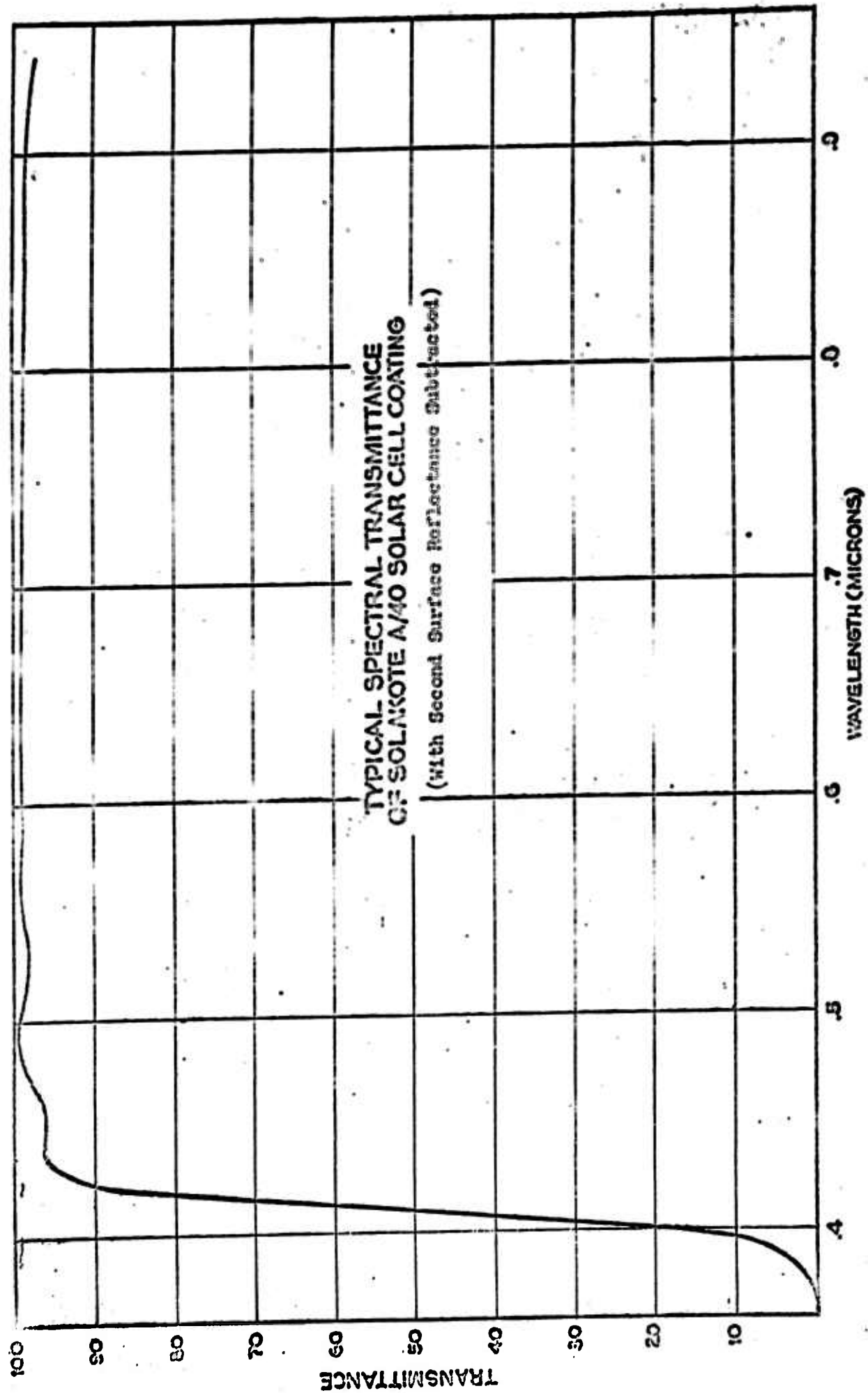


FIG. 8

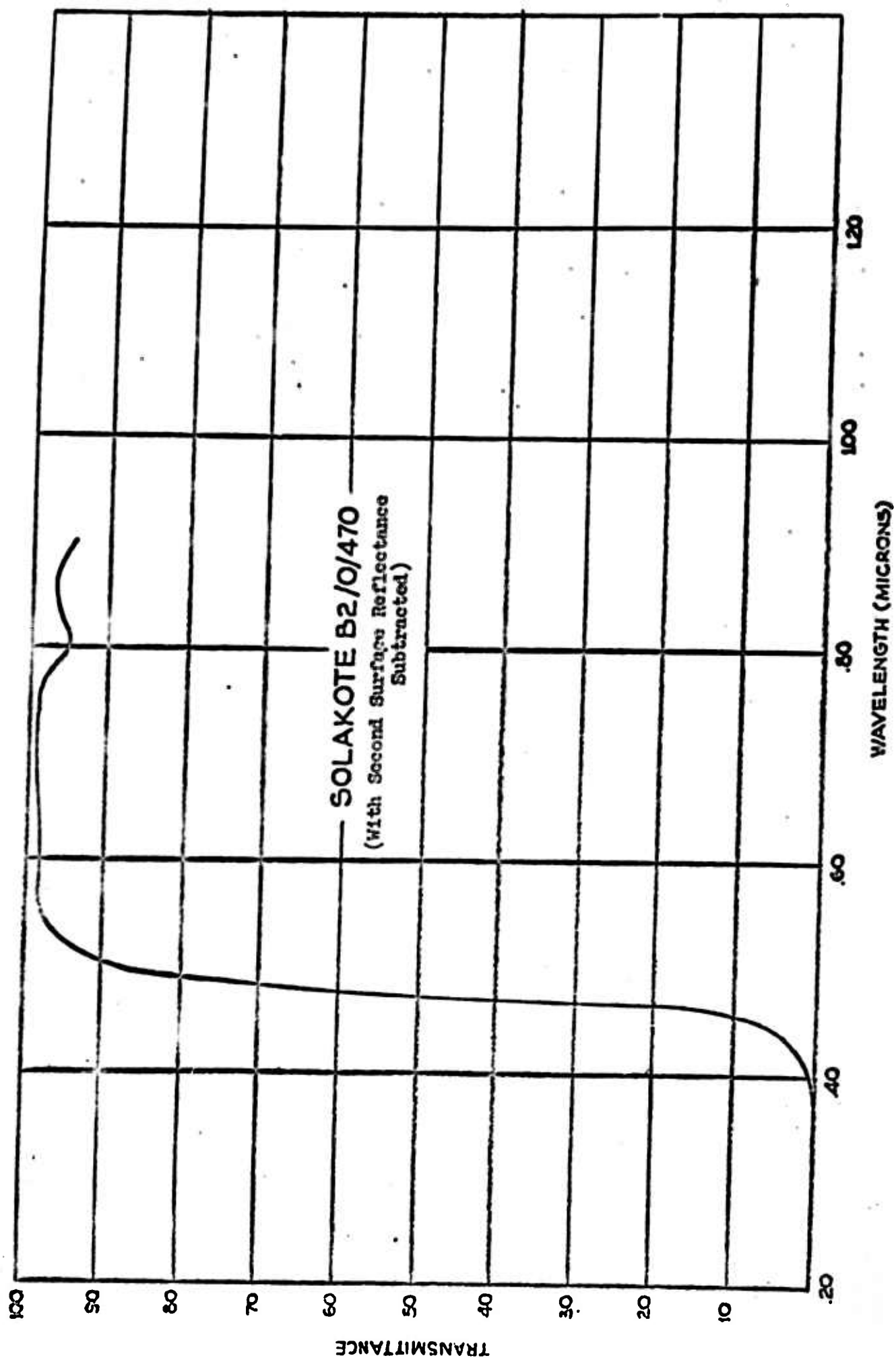


FIG. 9

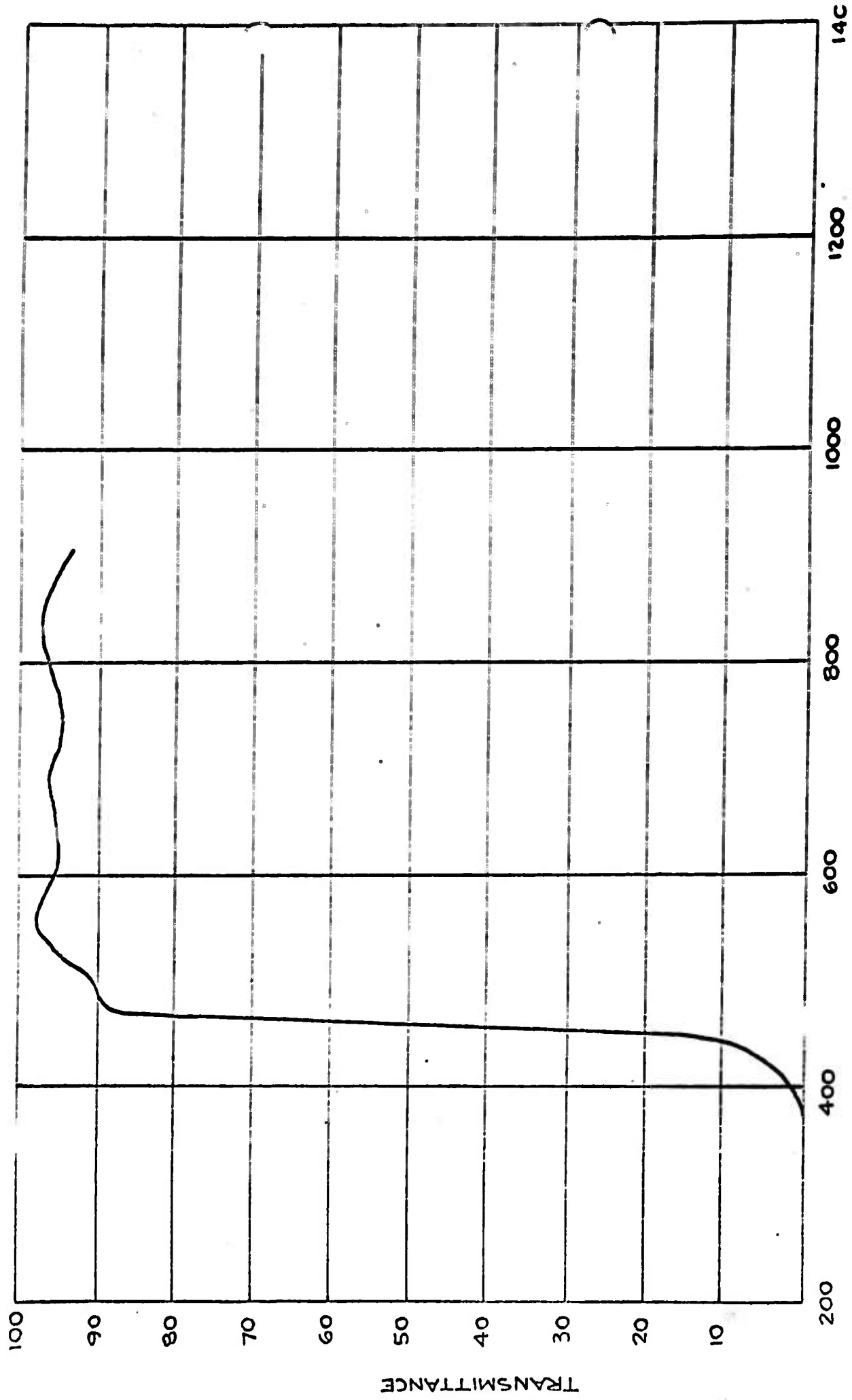


FIG. 10 OCL1 CELL COVER SLIP
TYPE 207 - SCC-160
(With Second Surface Reflectance Subtracted)

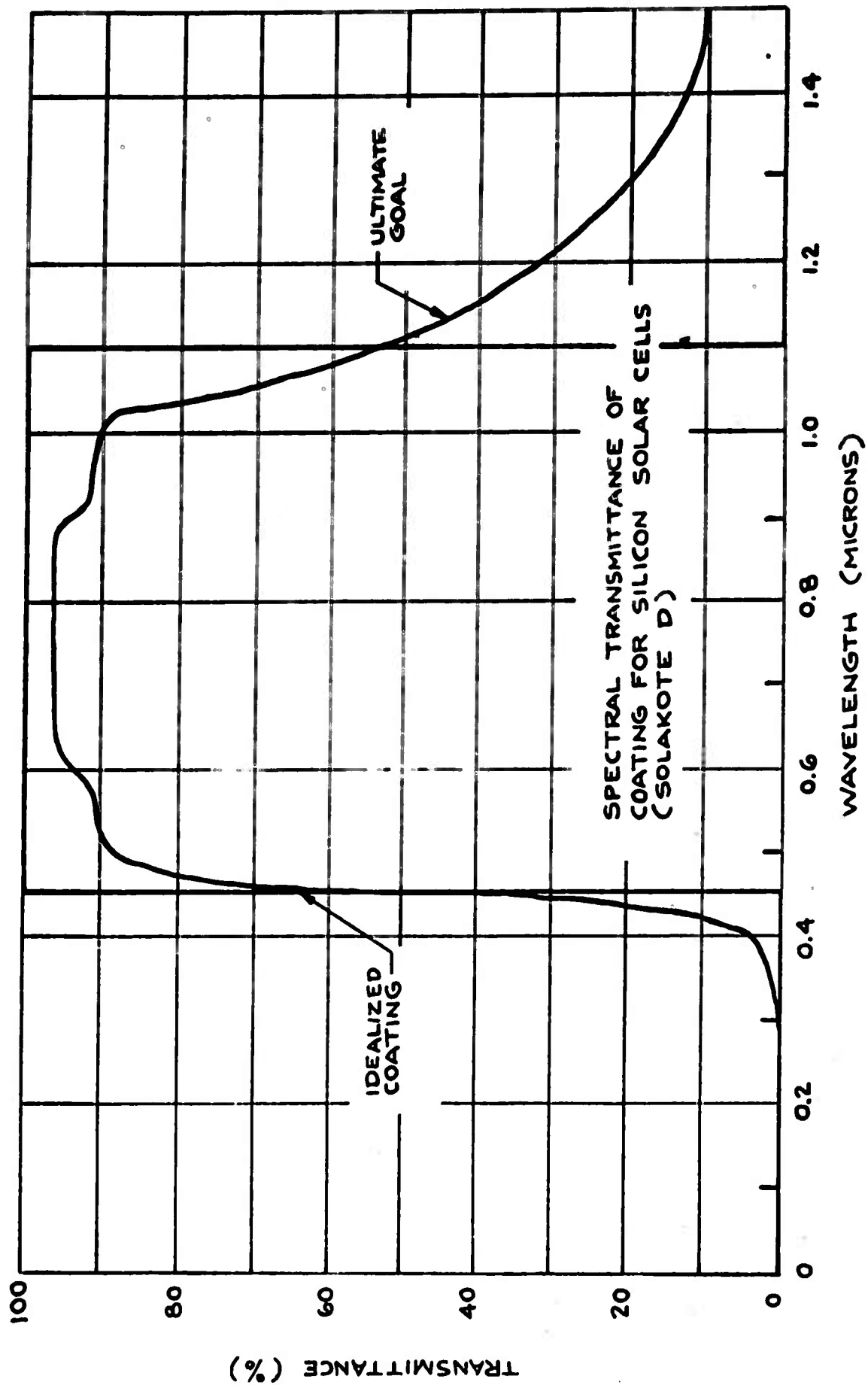


FIG.11

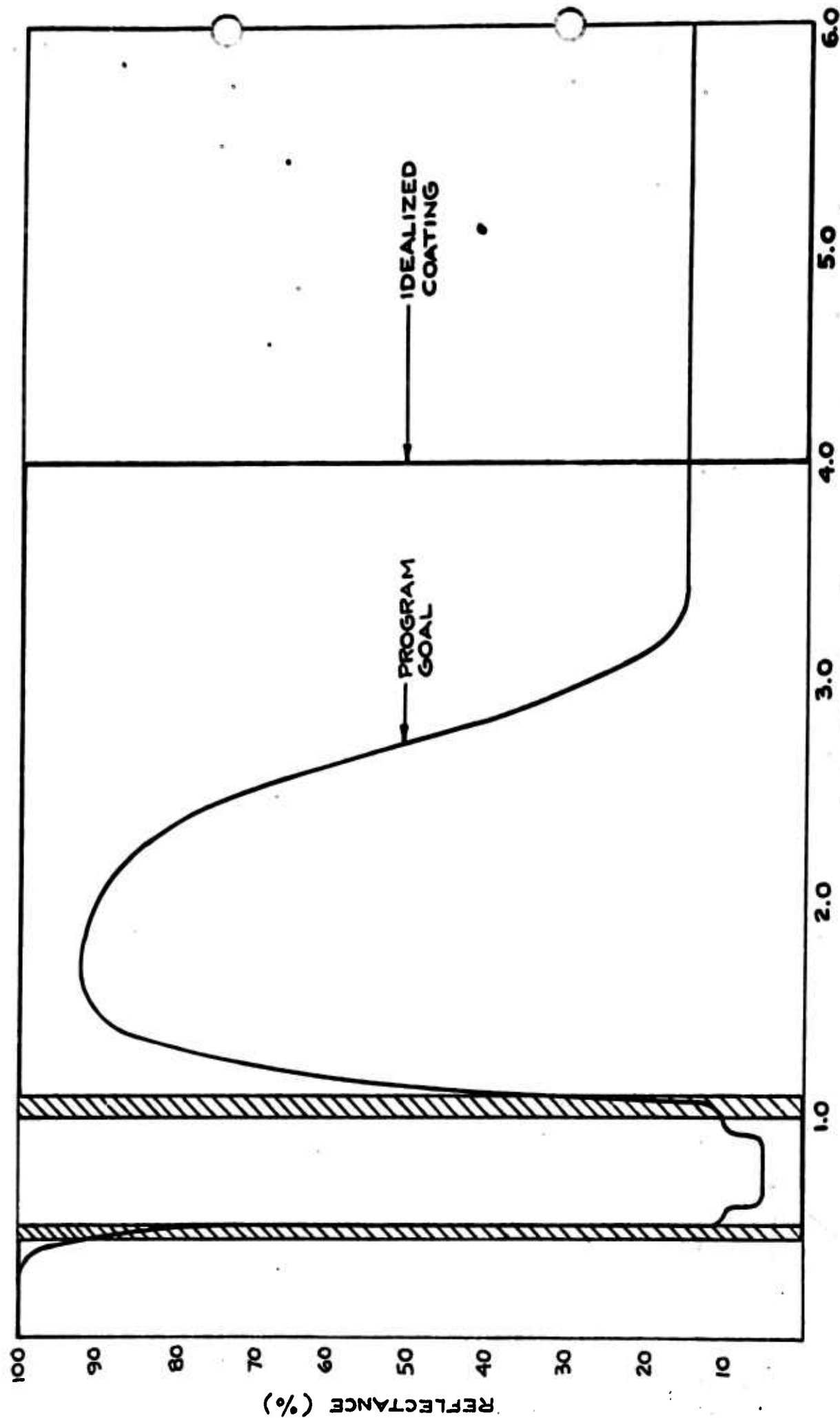


FIG.12 - SPECTRAL REFLECTANCE OF COATING FOR SILICON SOLAR CELLS.

SPECTRAL EMISSIVITY OF TYPICAL SILICON
SOLAR CELL WITH SOLAKOTE A, B, C & D

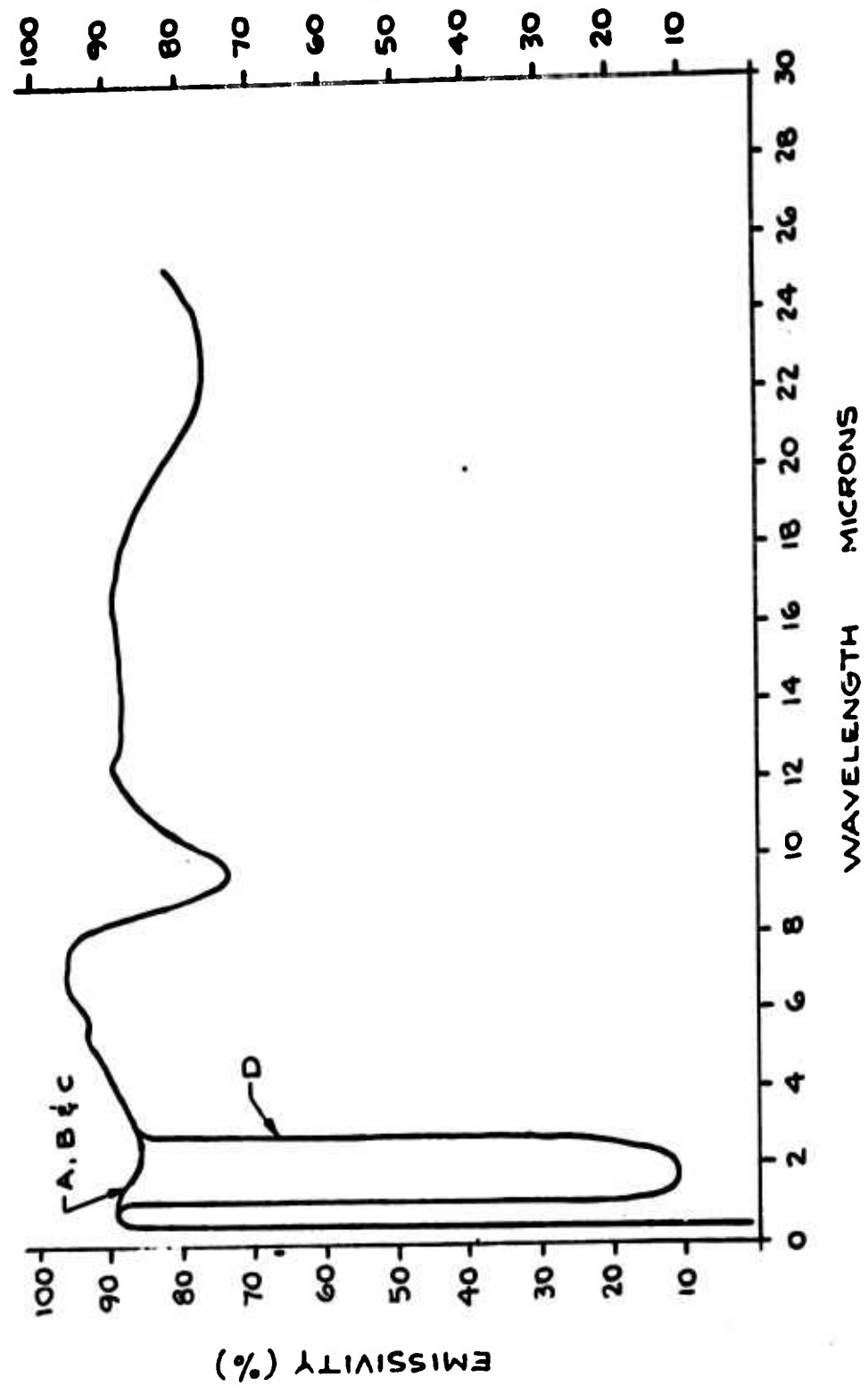


FIG. 13

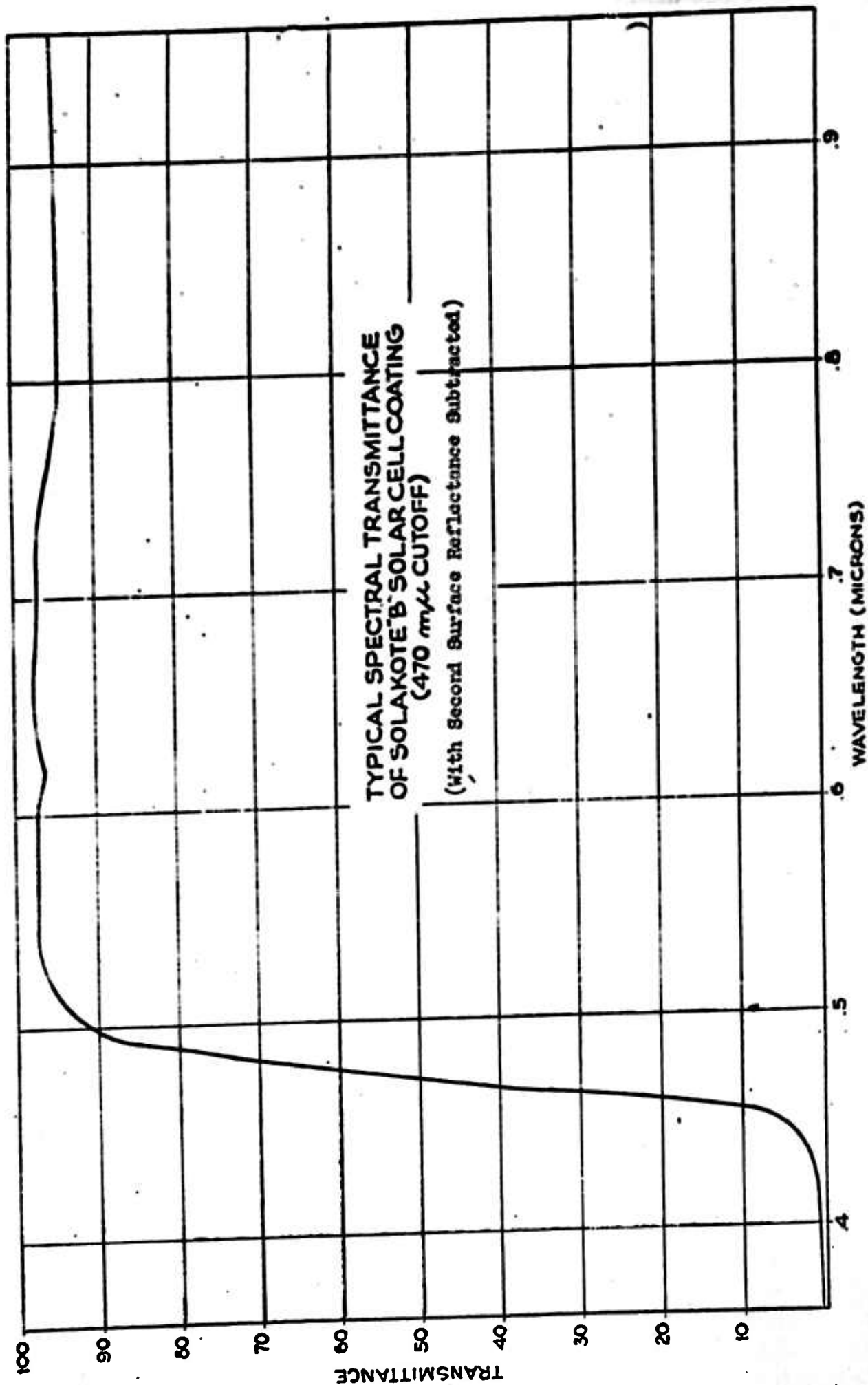


FIG. 14

**RELATIVE SPECTRAL SENSITIVITY
OF TYPICAL SILICON SOLAR CELL**

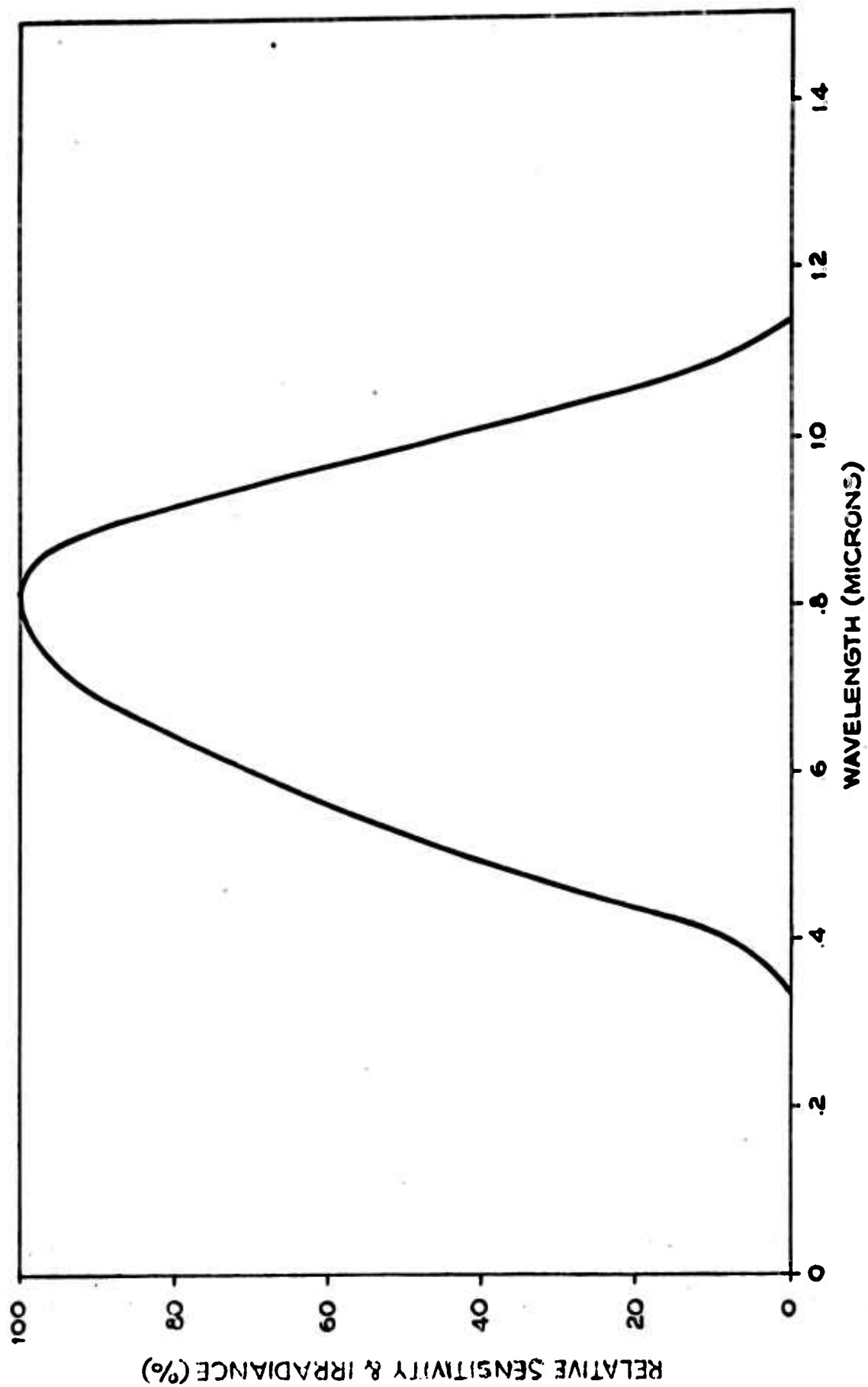
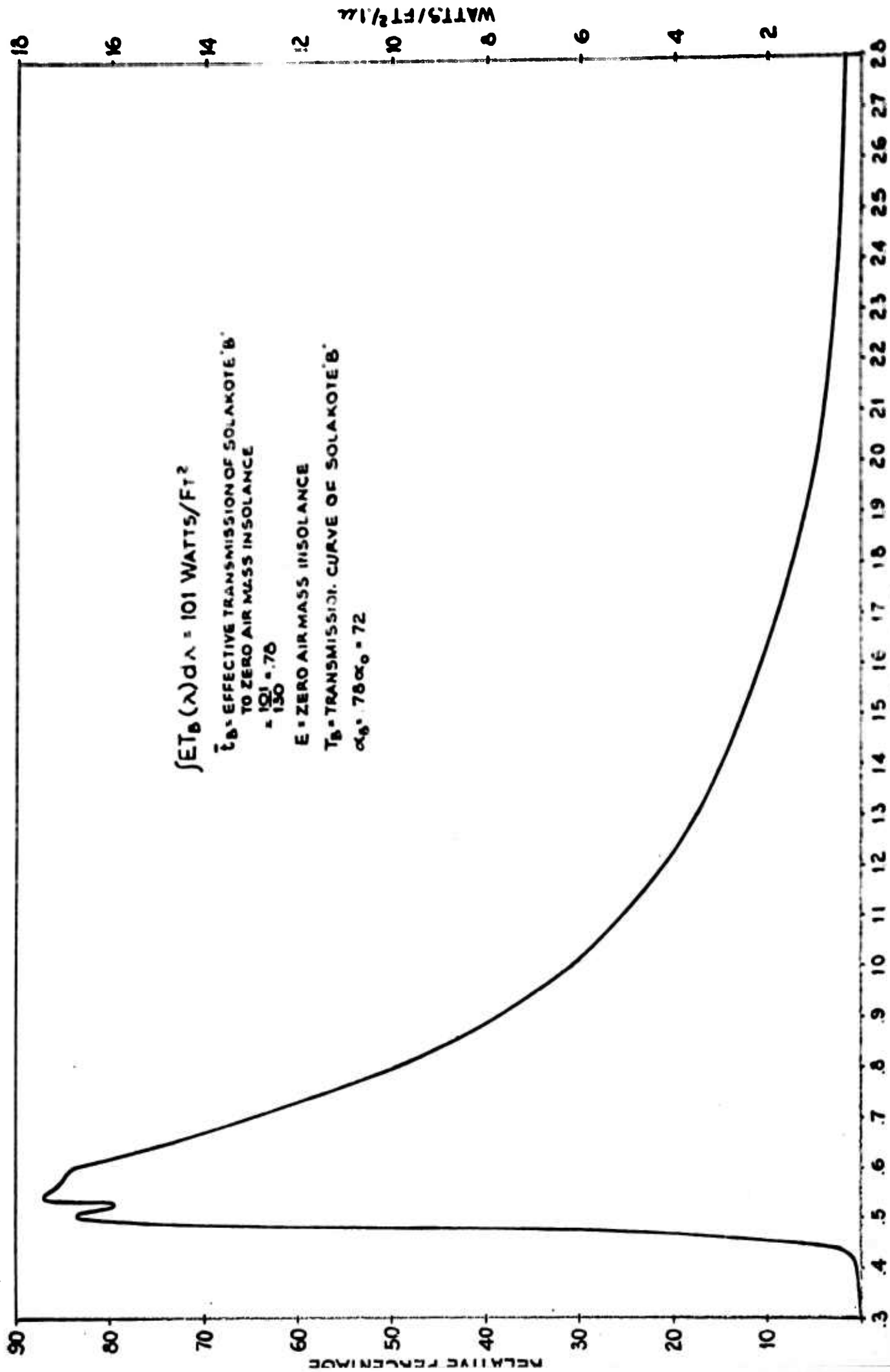


FIG.15



$$\int E T_B(\lambda) d\lambda = 101 \text{ WATTS/FT}^2$$

\bar{T}_B = EFFECTIVE TRANSMISSION OF SOLAKOTE 'B' TO ZERO AIR MASS INSOLANCE
 $= 101 \div 130$
 $= .76$

E = ZERO AIR MASS INSOLANCE

T_B = TRANSMISSION CURVE OF SOLAKOTE 'B'

$\alpha_0 = 78 \alpha_0 = 72$

FIG.16

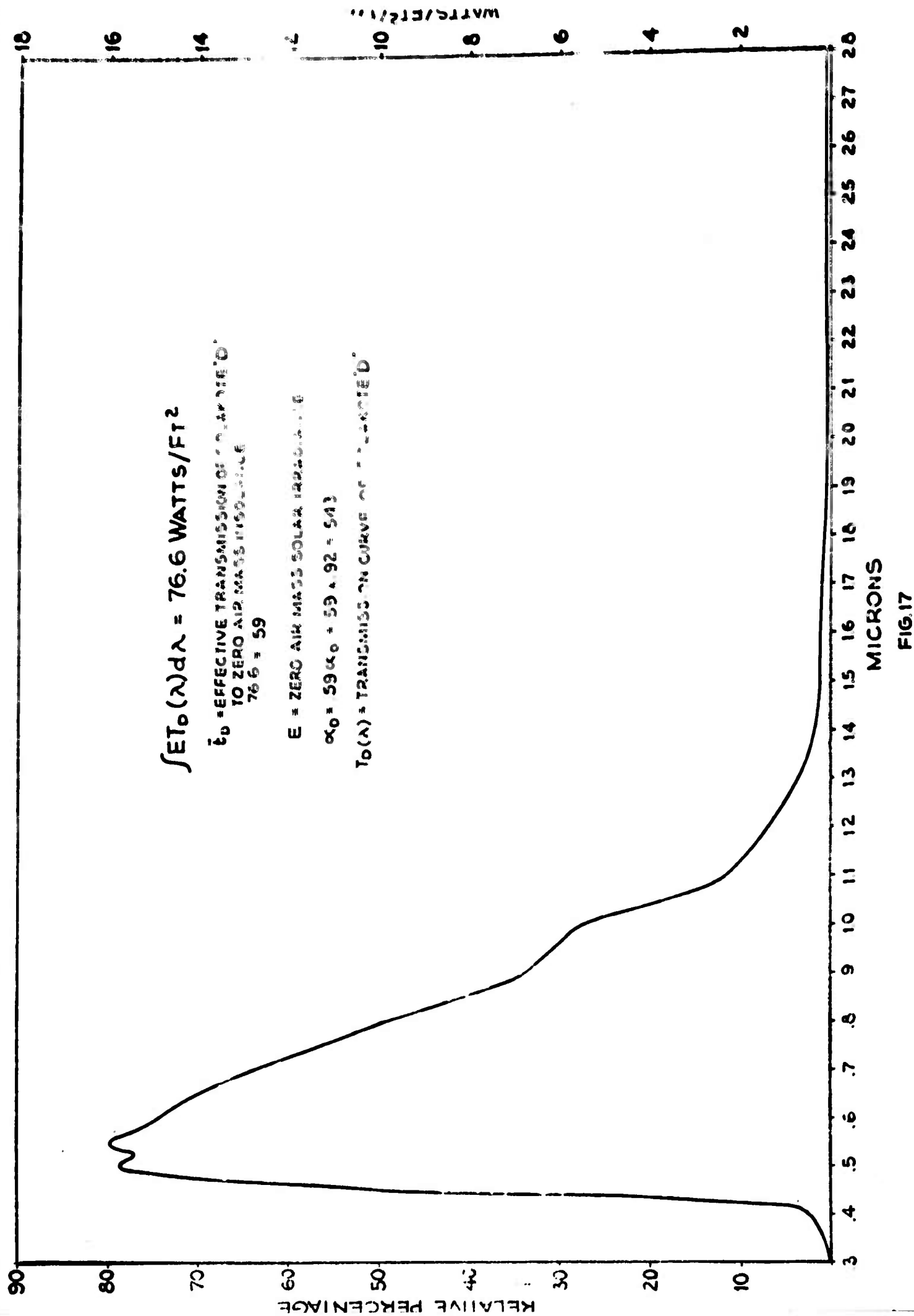
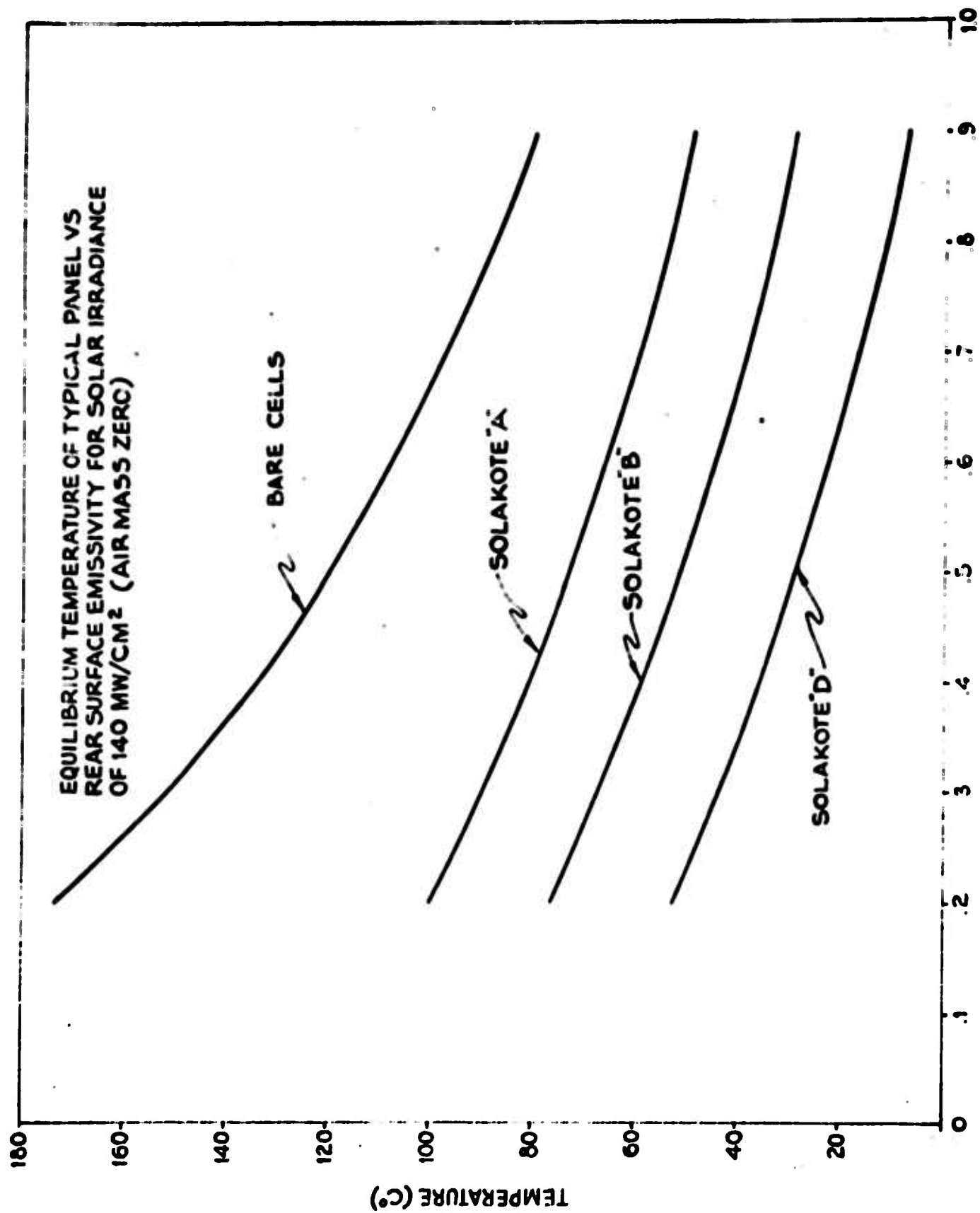


FIG.17



REAR SURFACE EMISSIVITY
FIG 18

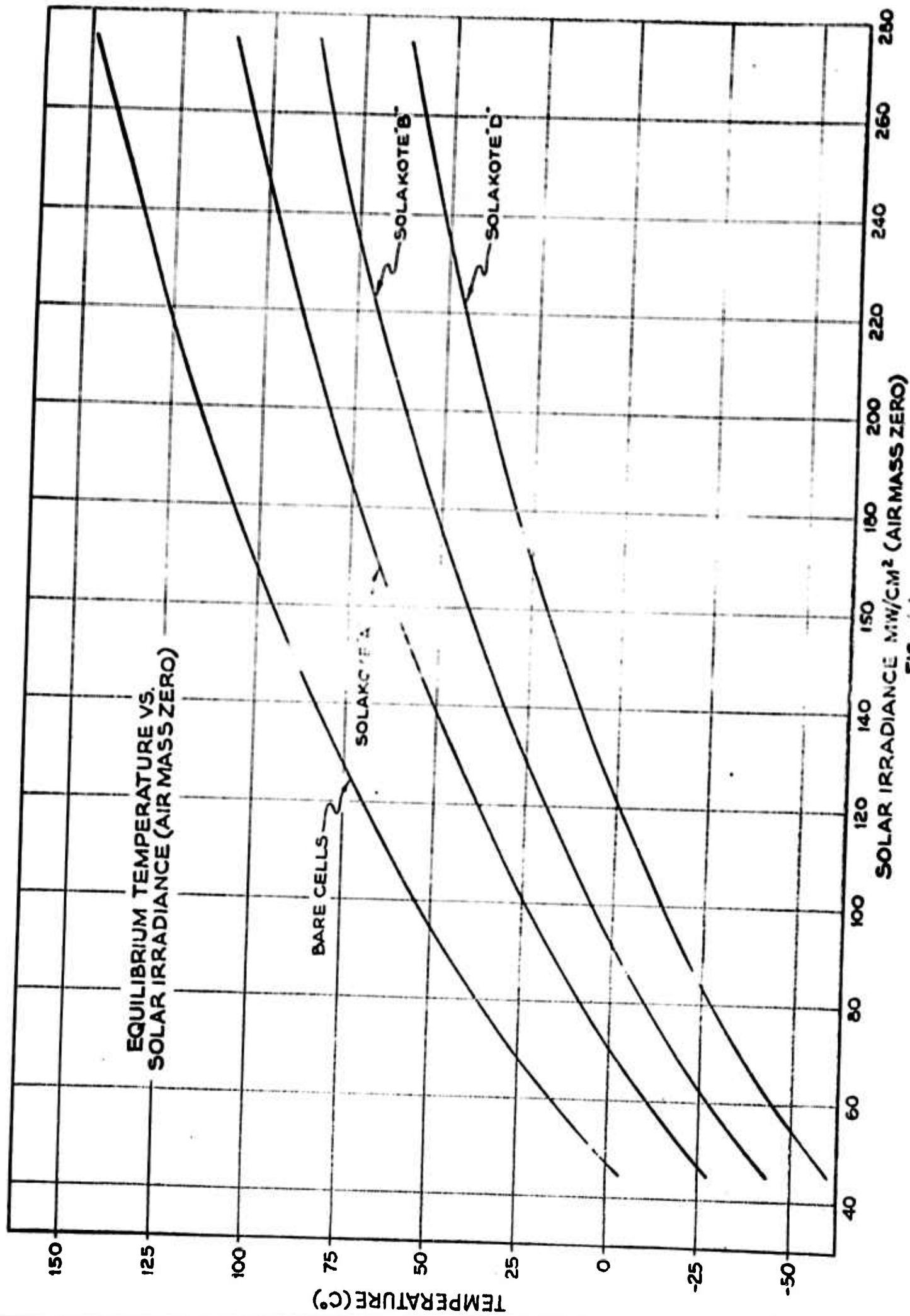


FIG. 1

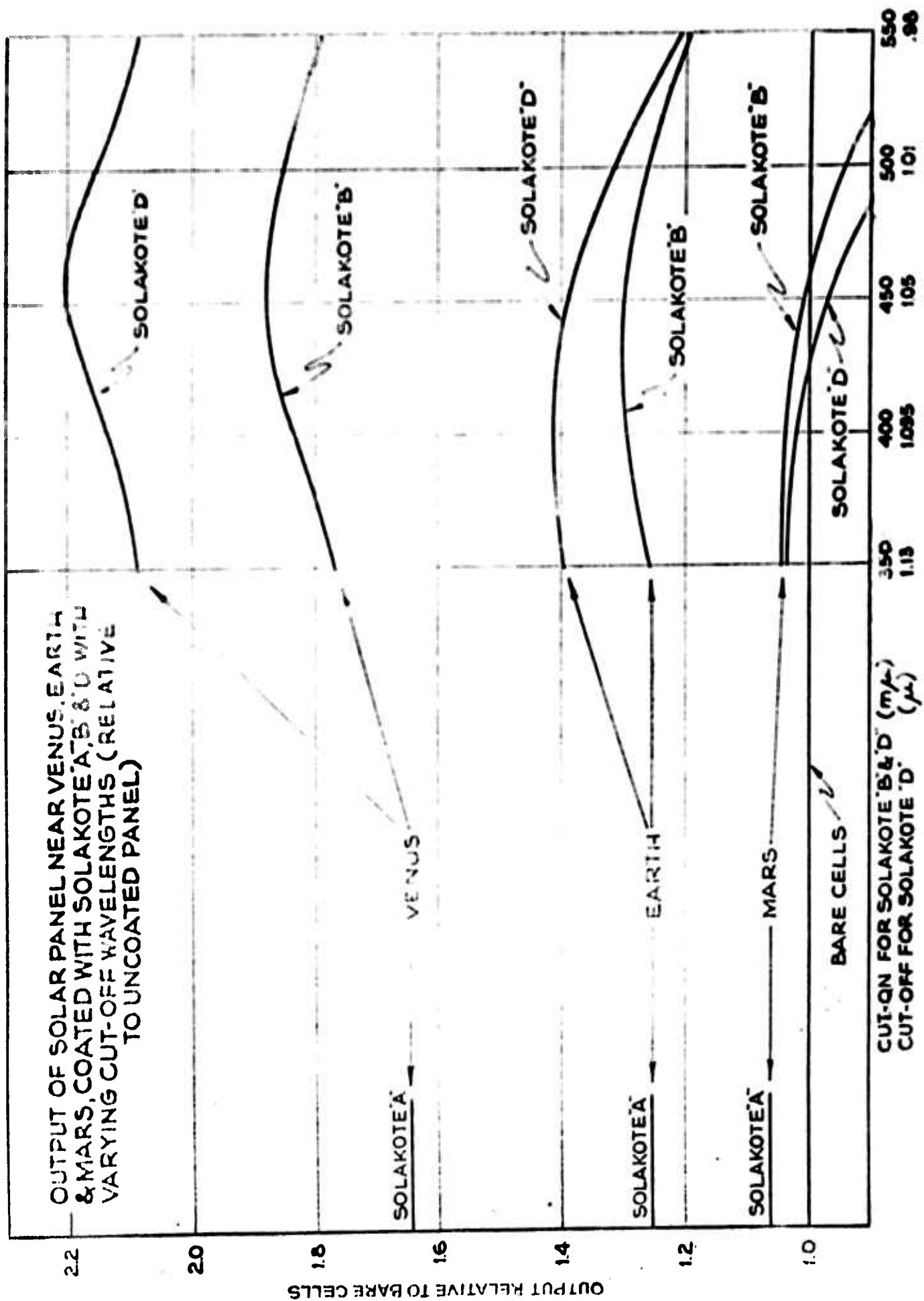


FIG. 20

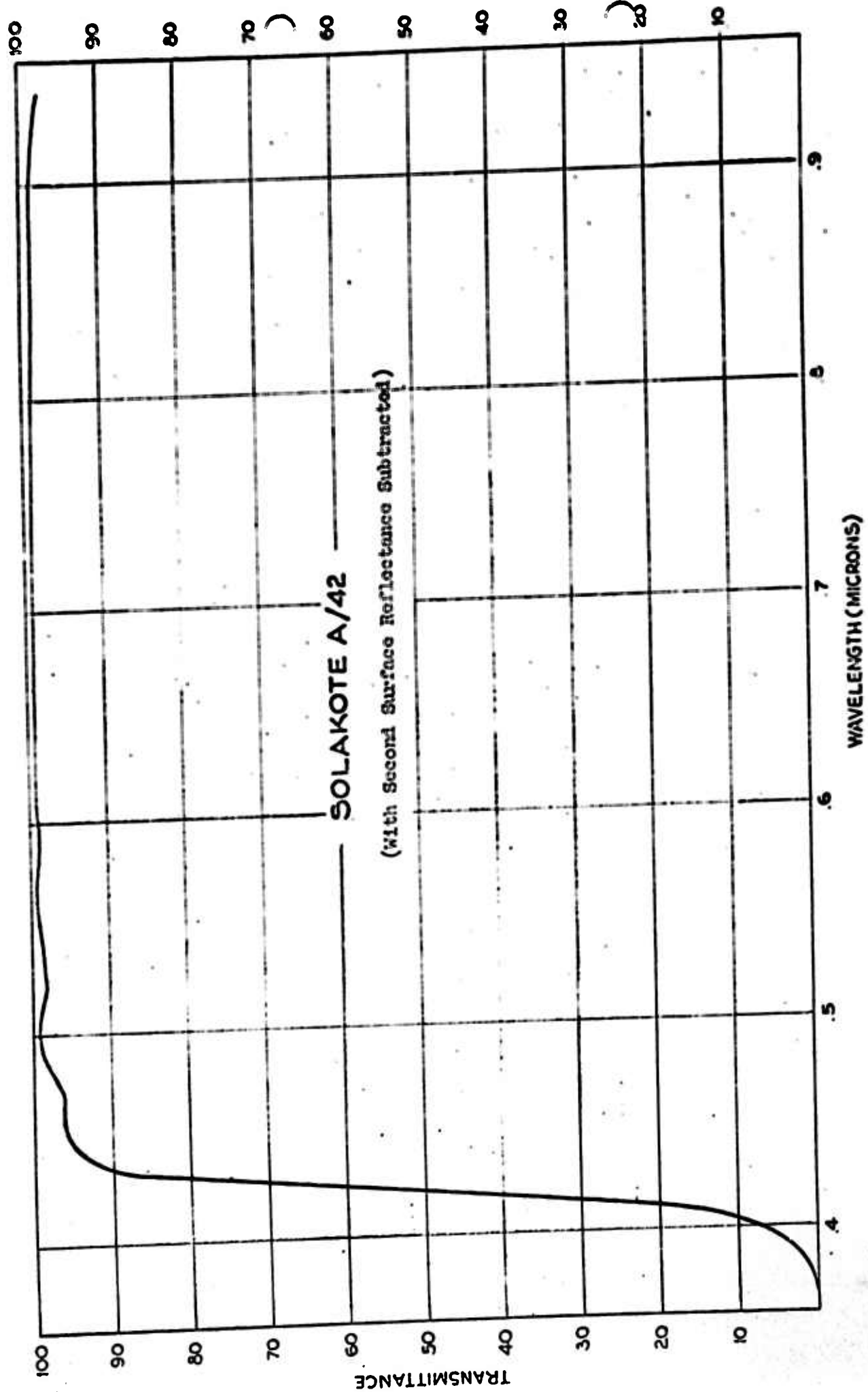


FIG. 21

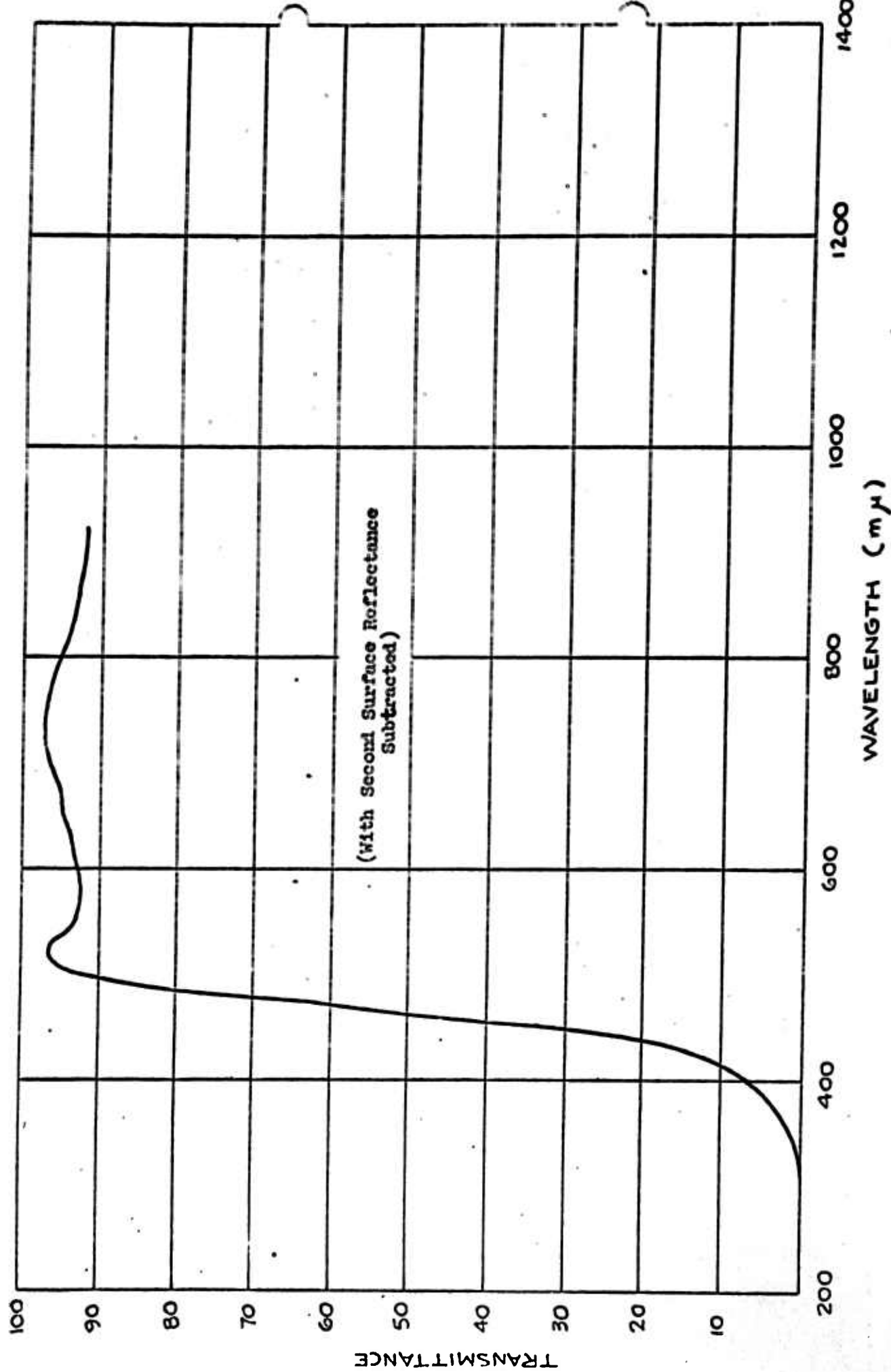
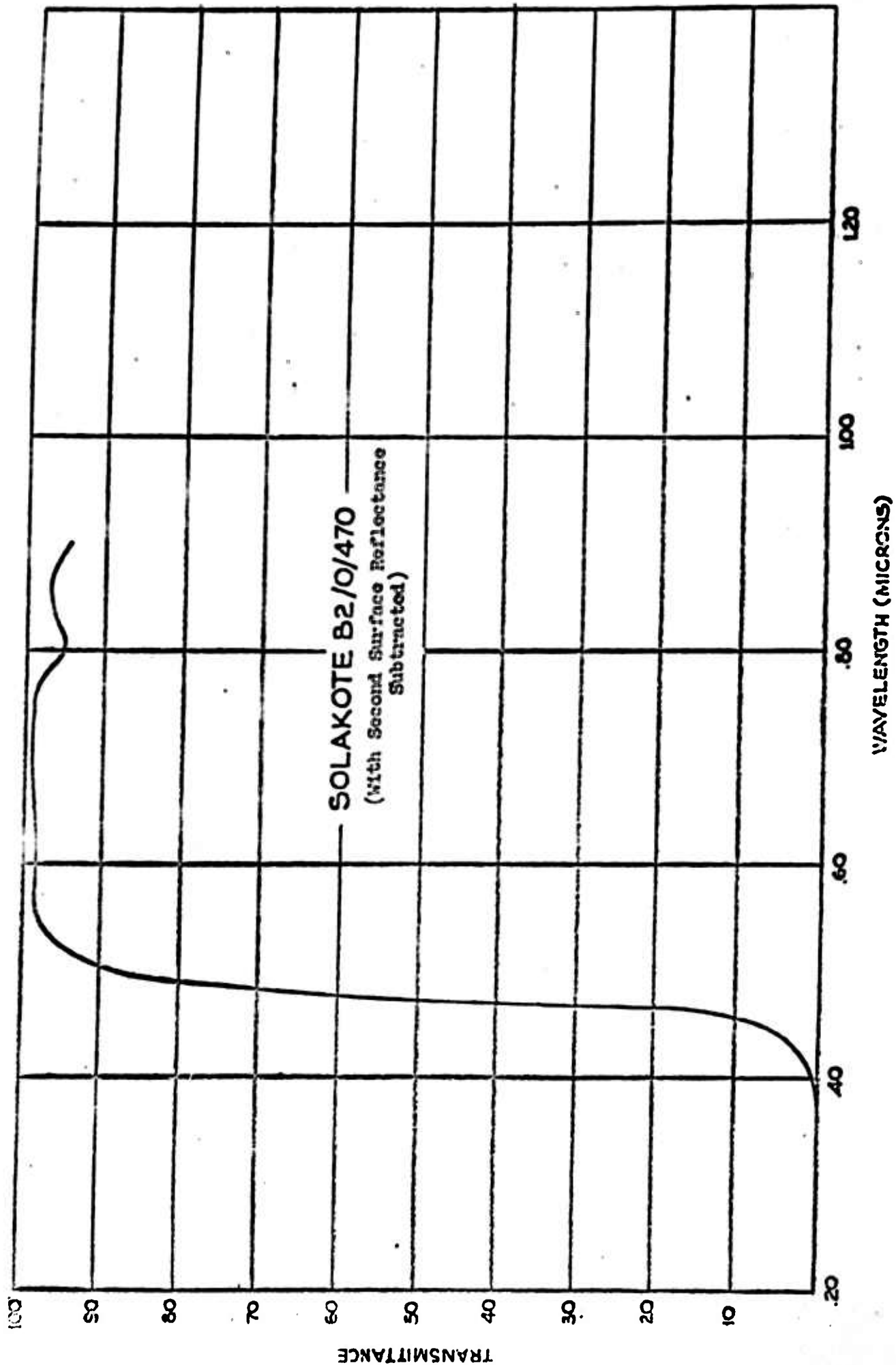


FIG. 22 SOLAKOTE BI/S/460



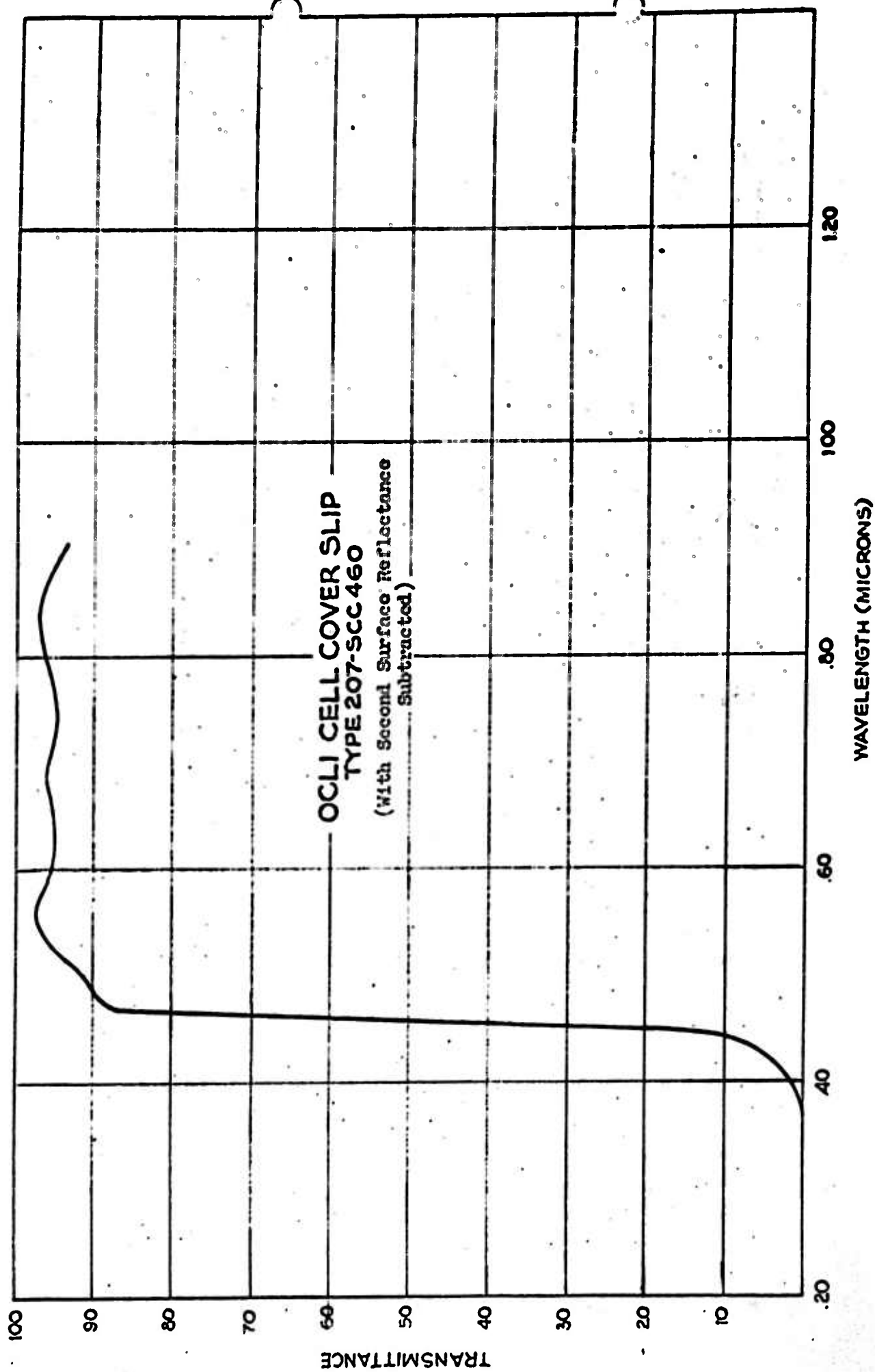


FIG 24

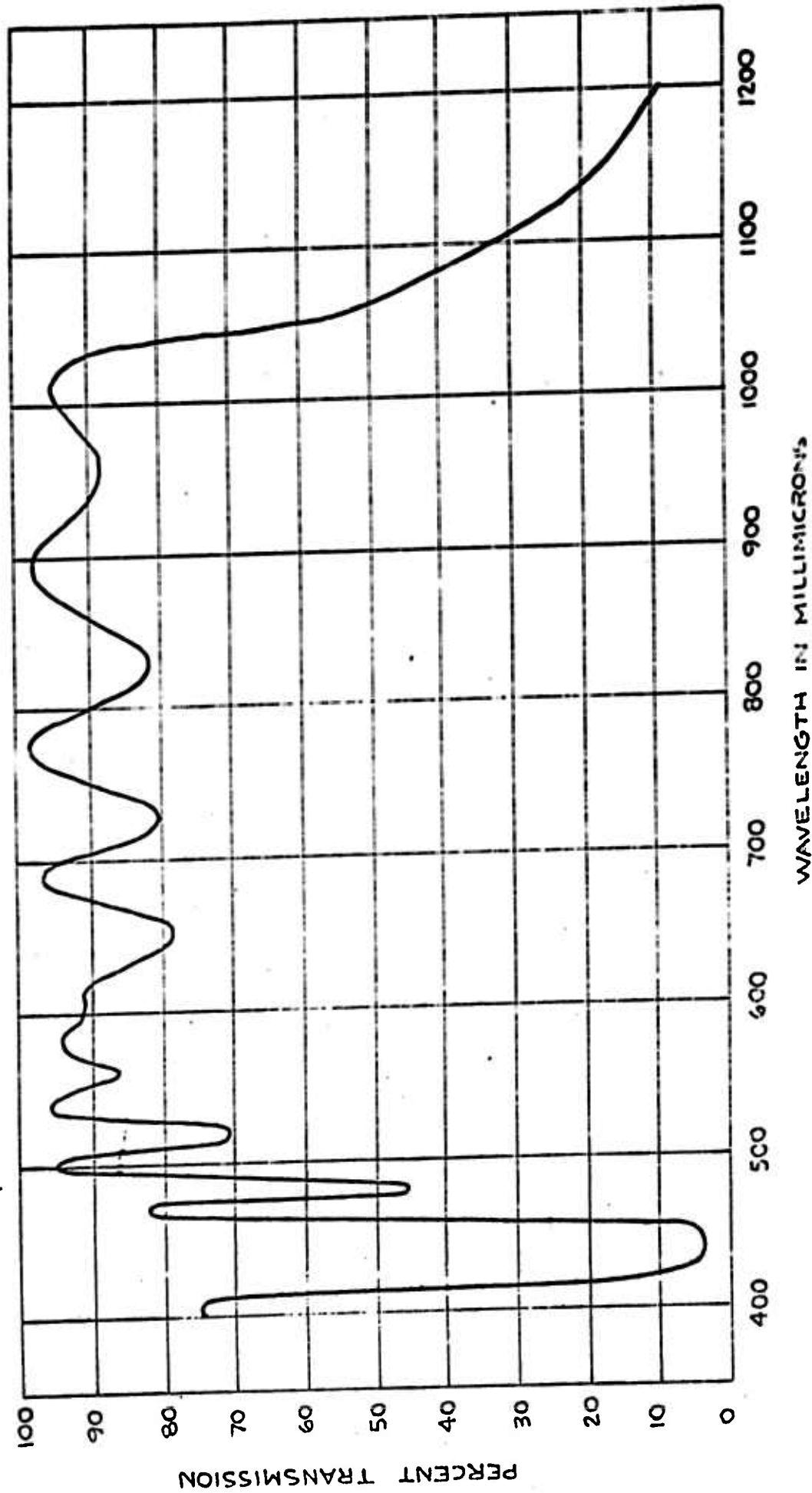


FIG. 25 FISH-SCHURMAN'S INFRA-RED REFLECTOR #3119
(with Second Surface Reflectance Subtracted)

PERCENT REFLECTION

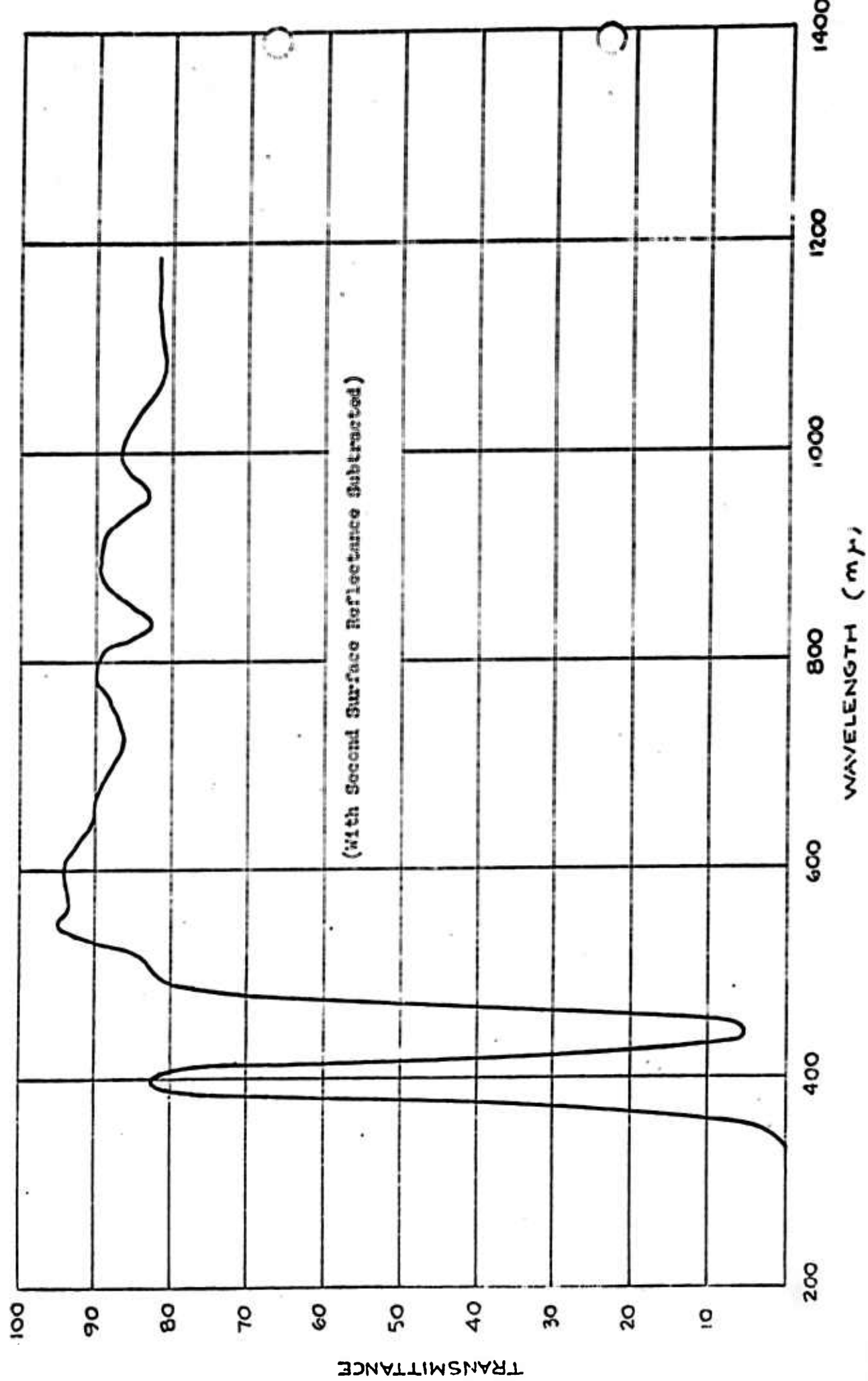


FIG. 26 FISH - SCHURMAN CELL COATING, TYPE 3119

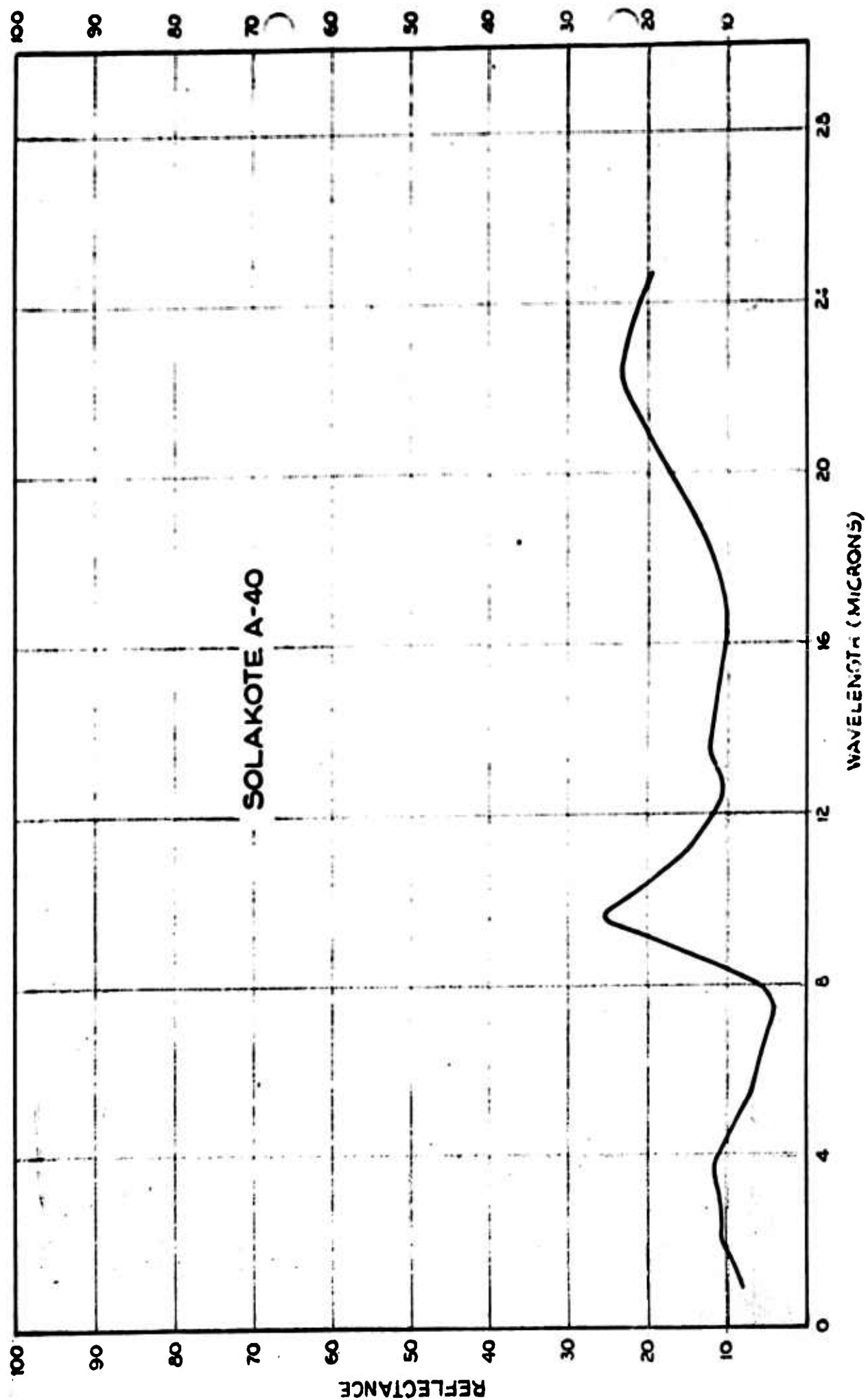


FIG. 27

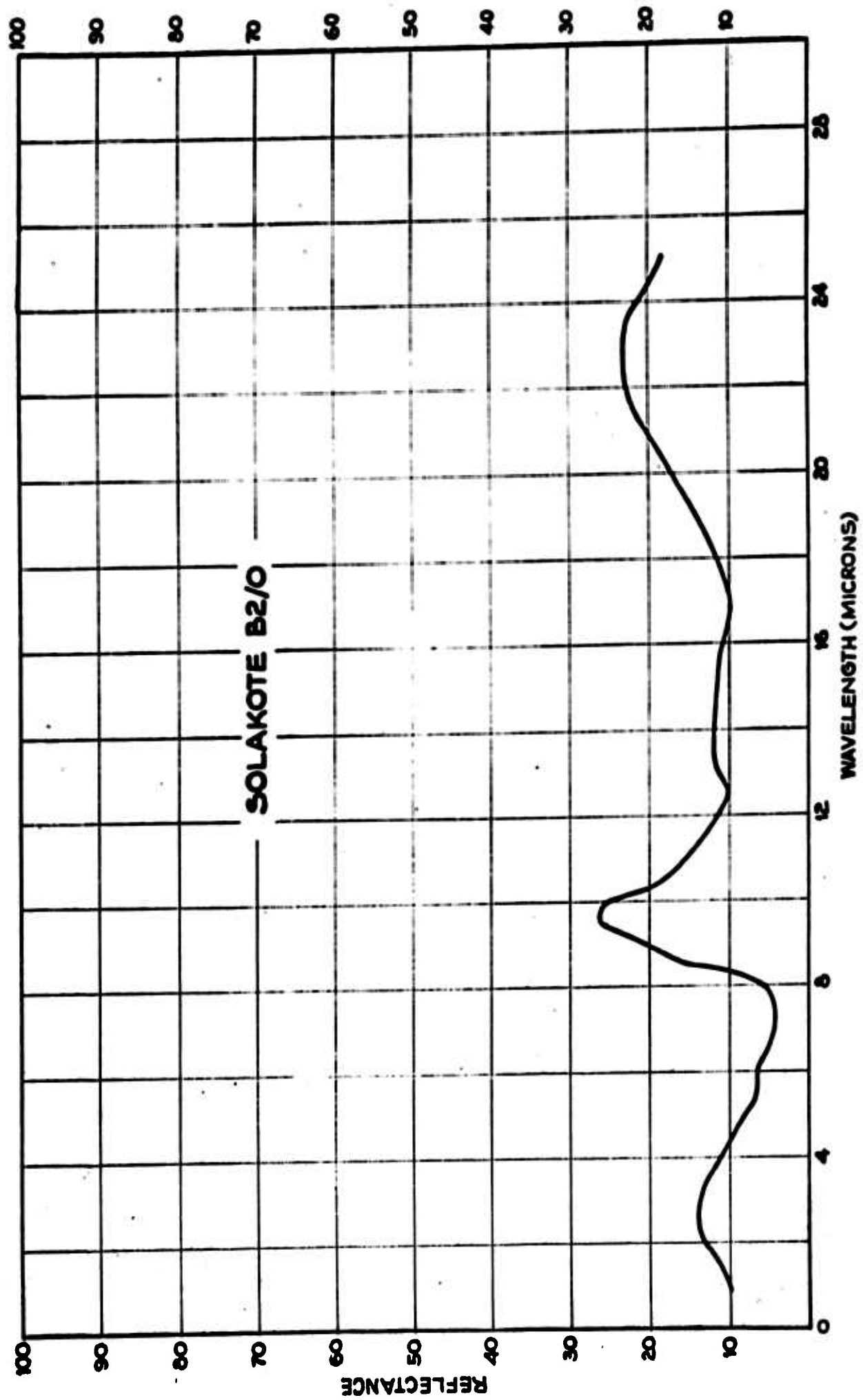


FIG. 26

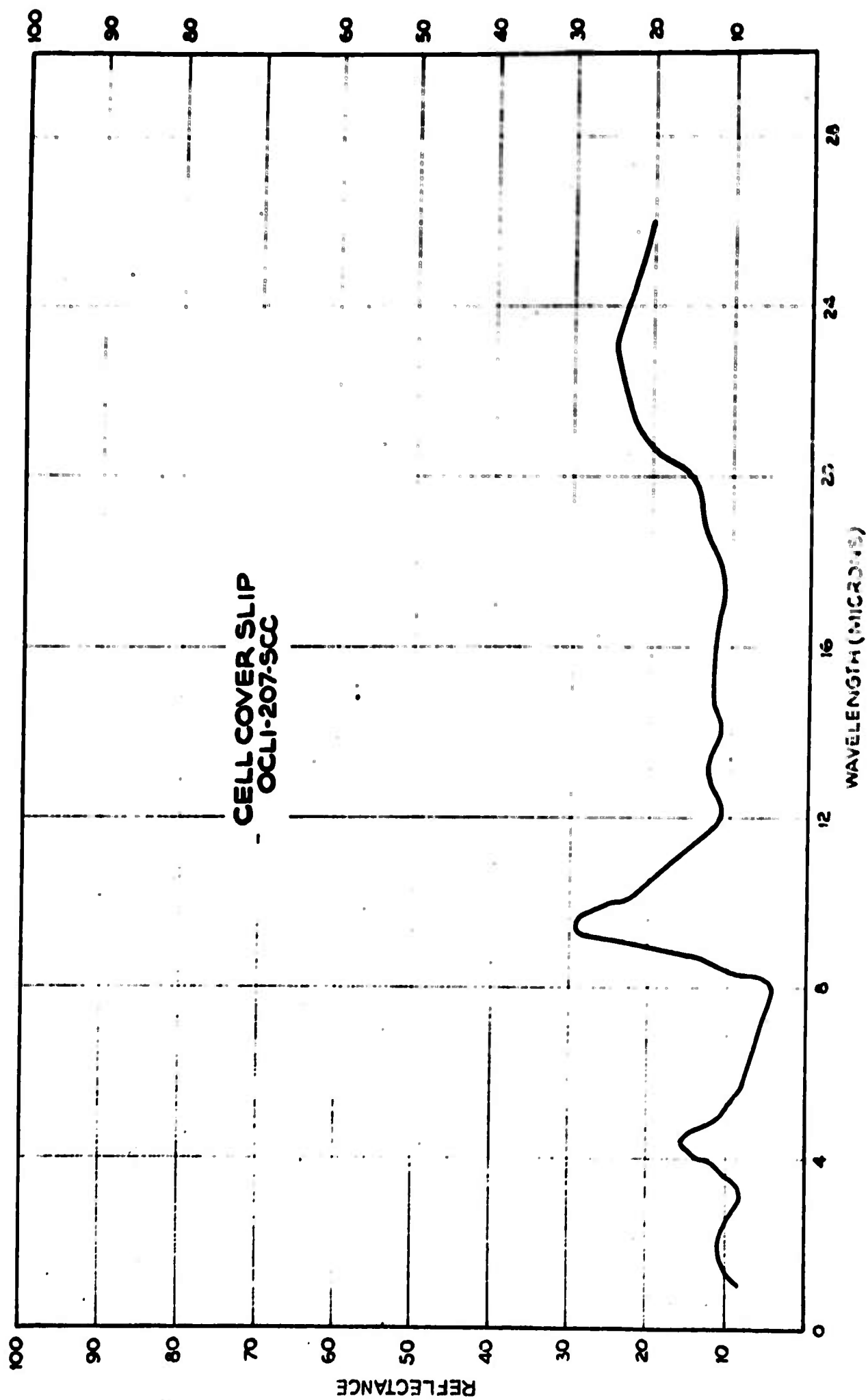
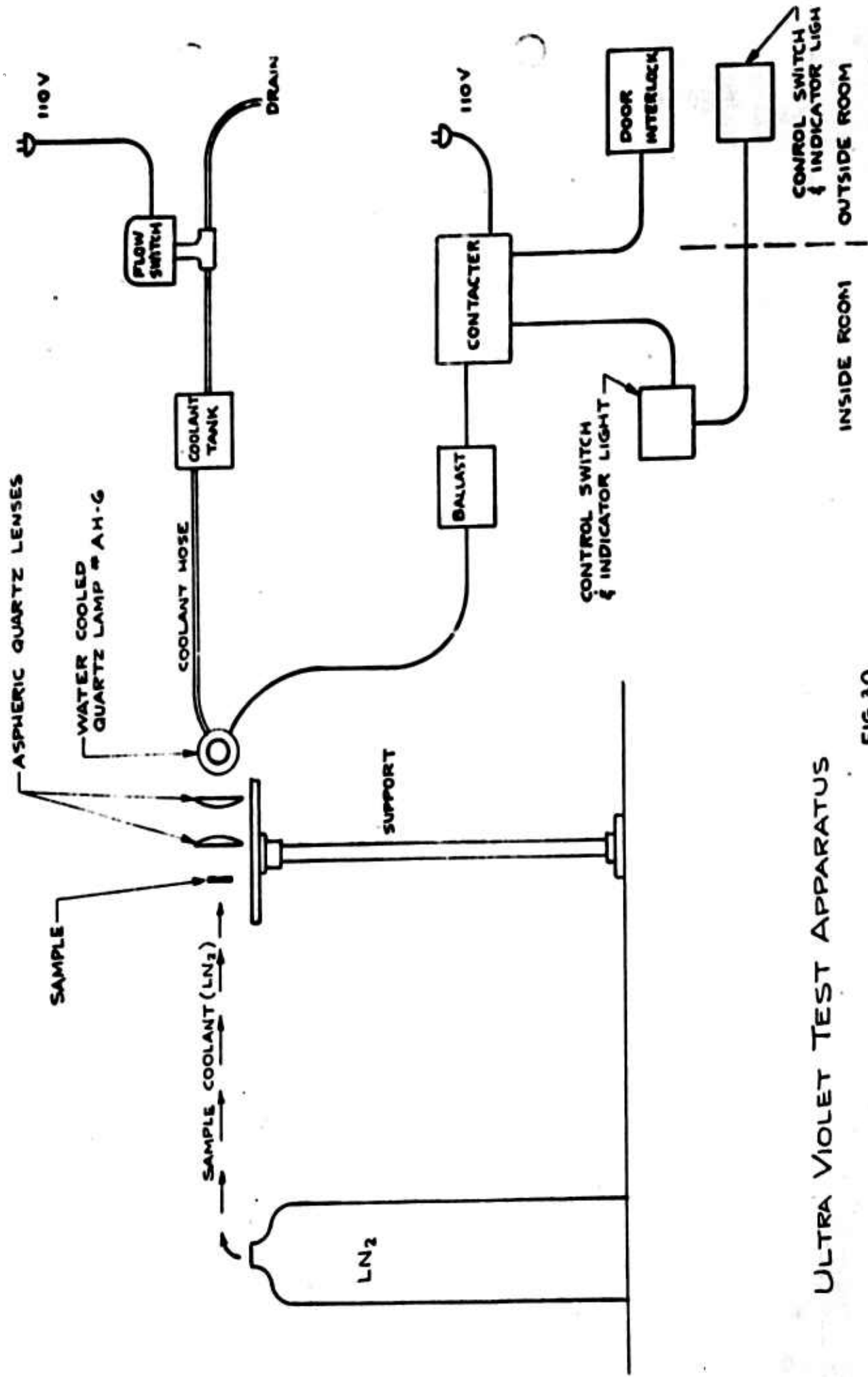


FIG. 29



ULTRA VIOLET TEST APPARATUS

FIG. 30

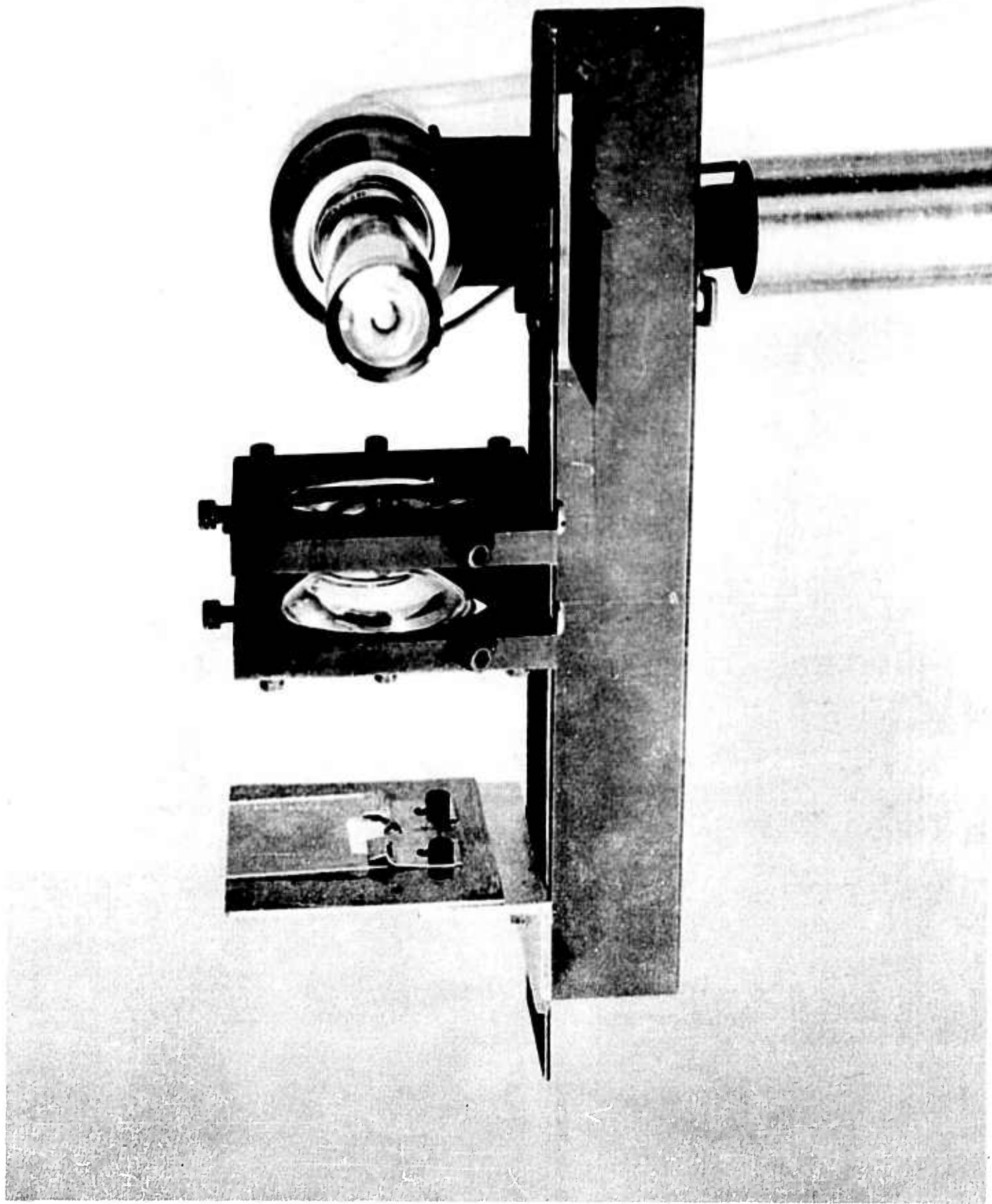


Figure 31. Ultraviolet Irradiation Test Apparatus



Figure 32. Typical Panel After Completion of Test Sequence

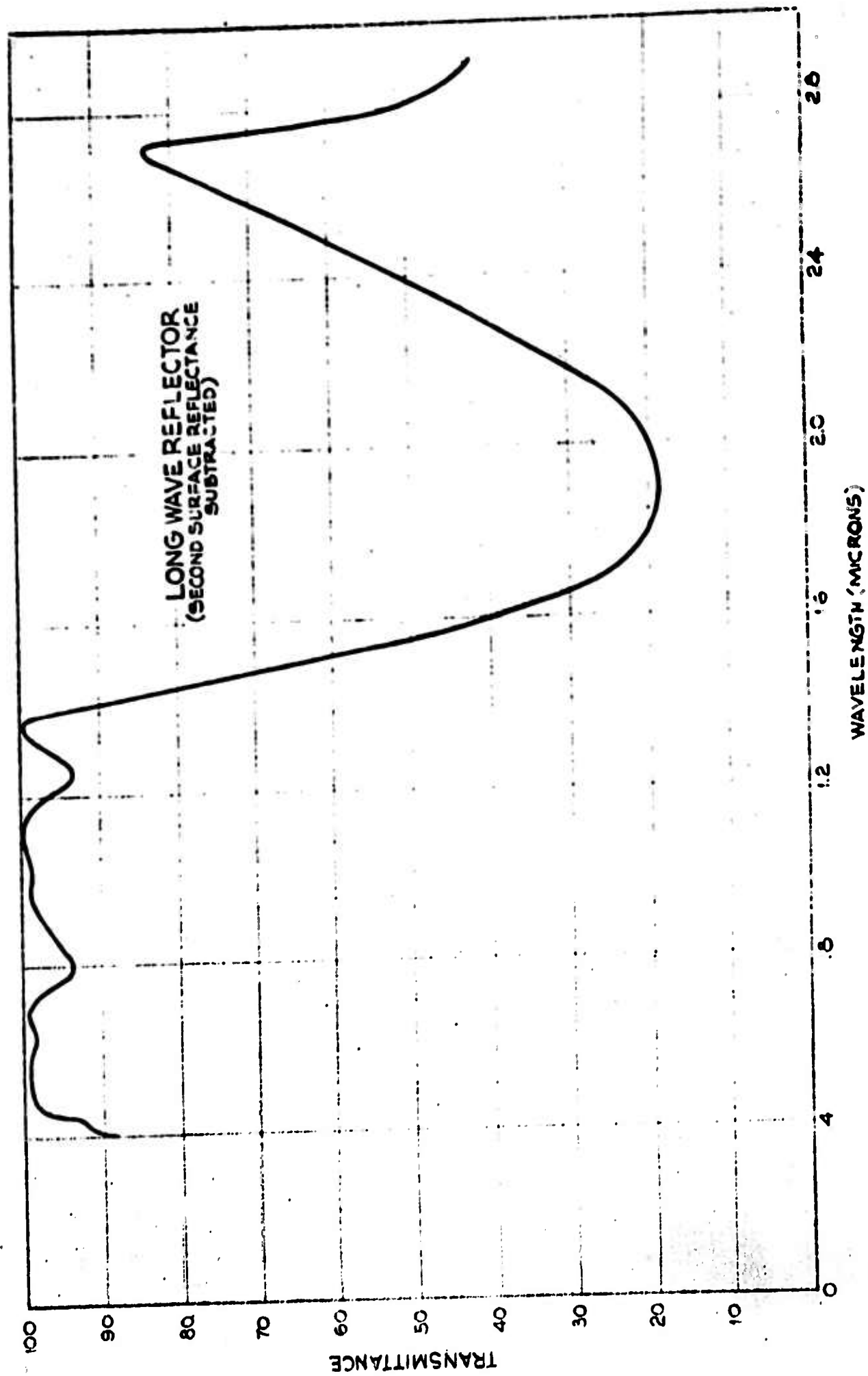
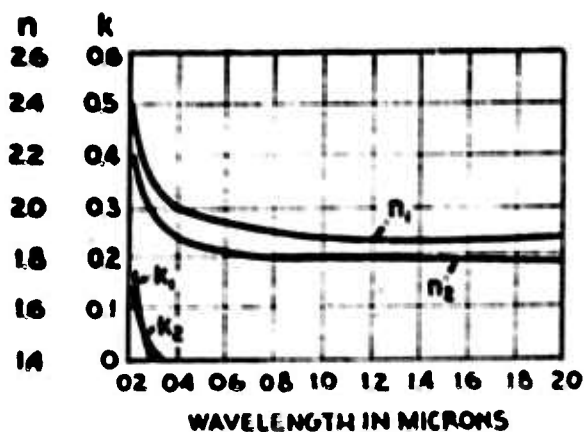
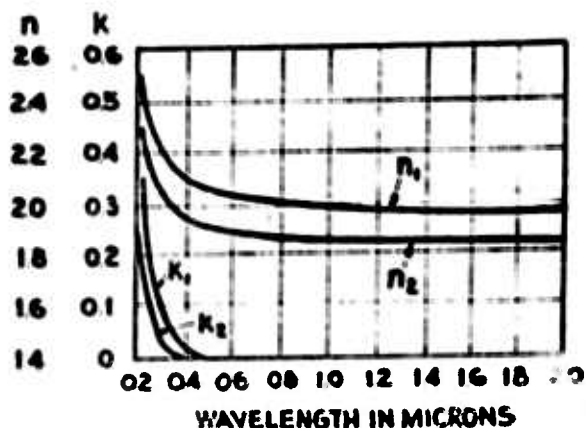


FIG 34



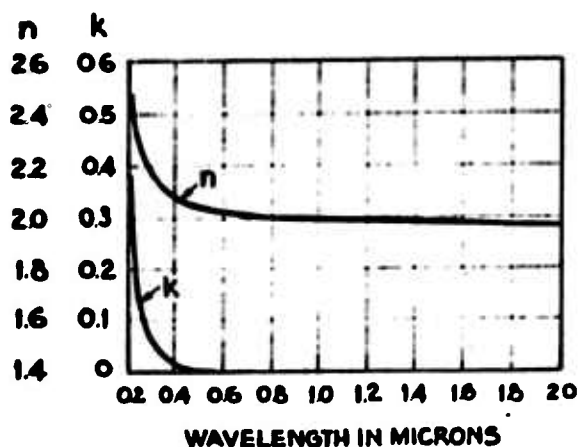
A - REFRACTIVE INDEX n AND ABSORPTION COEFFICIENT k OF UNBAKED La_2O_3 FILMS DEPOSITED AT 300°C SUBSTRATE TEMP. SUBSCRIPT 1 CORRESPONDS TO FILMS $3/4$ WAVELENGTH THICK AT 0.5 MICRON, SUBSCRIPT 2 TO THOSE $1/4$ WAVELENGTH THICK AT THE SAME WAVELENGTH

REF: HASS JOS A 49 118 (1959)



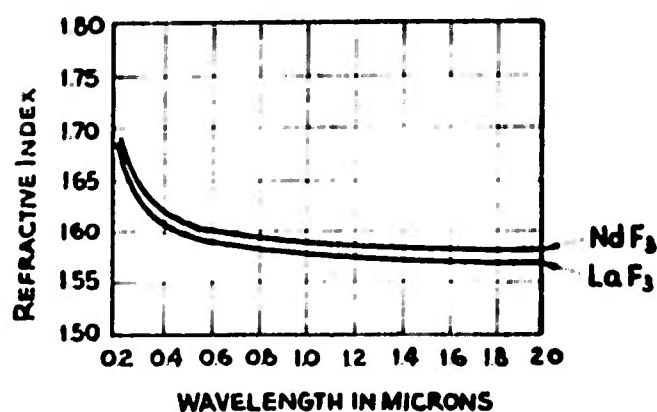
B - REFRACTIVE INDEX n AND ABSORPTION COEFFICIENT k OF UNBAKED Pt_6O_{11} FILMS DEPOSITED AT 300°C SUBSTRATE TEMP. SUBSCRIPT 1 CORRESPONDS TO FILMS $3/4$ WAVELENGTH THICK AT 0.5 MICRON, SUBSCRIPT 2 TO THOSE $1/4$ WAVELENGTH THICK AT THE SAME WAVELENGTH

REF: HASS JOS A 49 2 119 (1959)



C - REFRACTIVE INDEX n AND ABSORPTION COEFFICIENT k OF UNBAKED Nd_2O_3 FILMS DEPOSITED AT 300°C SUBSTRATE TEMP. BOAT CURRENT: 600 AMPERES. DEPOSITION RATE: 15 ANGSTROMS PER SECOND.

REF: HASS JOS A 49 2 119 (1959)



D - REFRACTIVE INDEX n OF FILMS OF NdF_3 AND LaF_3 AS A FUNCTION OF THE WAVELENGTH. SUBSTRATE TEMP. DURING DEPOSITION: 300°C .

REF: HASS JOS A 49 2 120 (1959)

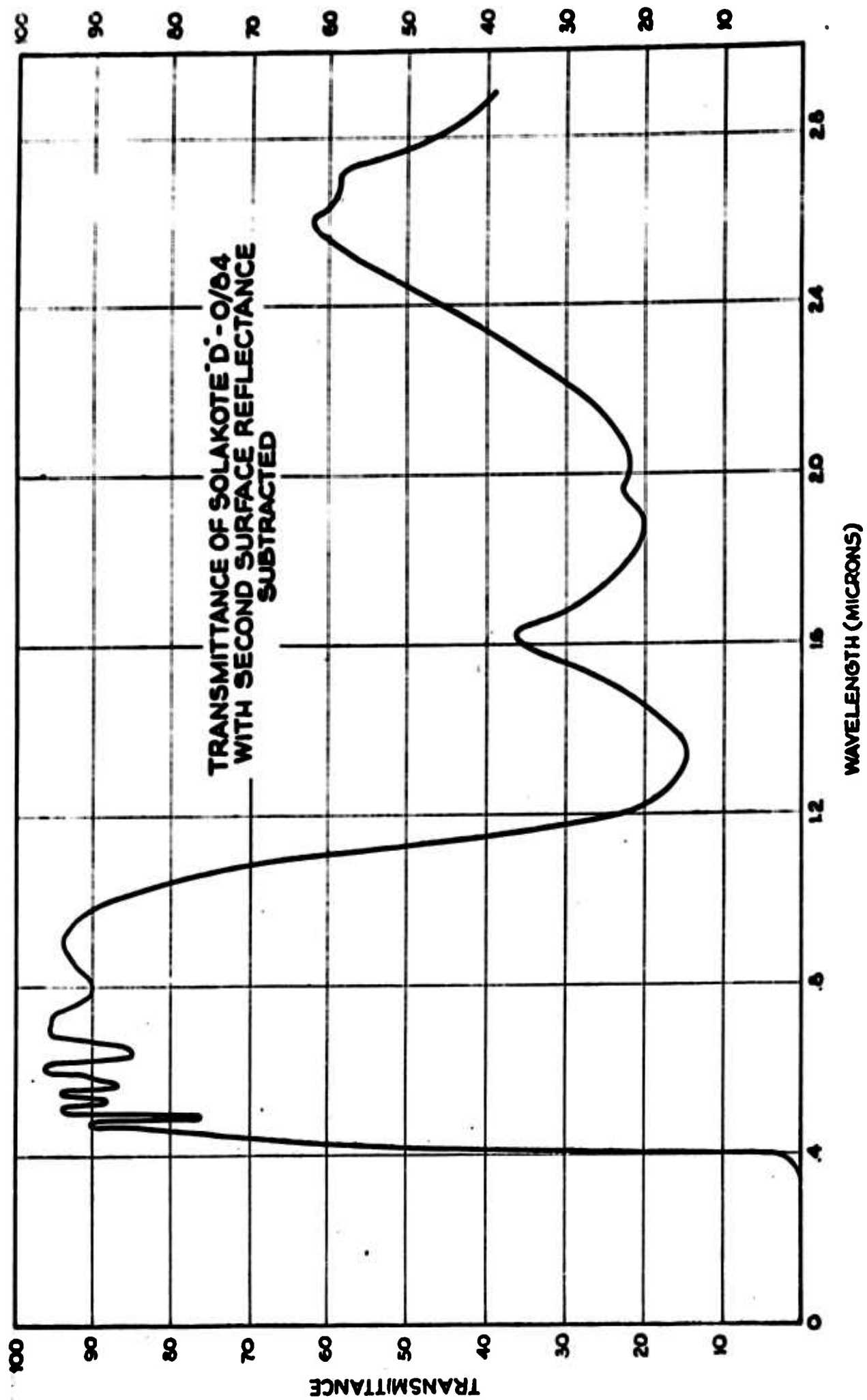


FIG. 6

DISSEMINATION LIST

Through Semi-Annual Report
AFSA Order No. 80-51
DISSEMINATION

Armed Services Technical Information Agency
Jenkins Hall Station
Jenkins Hall, Virginia
AFSA: AFSA

(3)

Commanding Officer
U. S. Army Signal A and D Laboratory
Fort Monmouth, New Jersey

AFSA: SIGRA/SL-P
AFSA: SIGRA/SL-ADJ
AFSA: Director of Research
AFSA: Tech Document Center
AFSA: SIGRA/SL-PS

(1)
(1)
(1)
(1)
(81)

Power Information Center
Moore School Building
200 South 33rd Street
Philadelphia 4, Pennsylvania

(1)

UNCLASSIFIED

UNCLASSIFIED